$B \to V, A, T$ tensor form factors in the covariant light-front approach: Implications on radiative B decays

Hai-Yang Cheng[1,2] and Chun-Khiang Chua[3]

[1]*Institute of Physics, Academia Sinica, Taipei, Taiwan 115, Republic of China*
[2]*Physics Department, Brookhaven National Laboratory, Upton, New York 11973, USA*
[3]*Department of Physics, Chung Yuan Christian University, Chung-Li, Taiwan 320, Republic of China*

(Received 30 September 2009; published 4 June 2010)

We reanalyze the $B \to M$ tensor form factors in a covariant light-front quark model, where M represents a vector meson V, an axial-vector meson A, or a tensor meson T. The treatment of masses and mixing angles in the $K_{1A,1B}$ systems is improved, where K_{1A} and K_{1B} are the $^3P_1$ and $^1P_1$ states of the axial-vector meson K_1, respectively. Rates of $B \to M\gamma$ decays are then calculated using the QCD factorization approach. The updated $B \to K^*\gamma$, $B \to K_1(1270)\gamma$, $K_1(1400)\gamma$, and $K_2\gamma$ rates agree with the data. The $K_1(1270)$–$K_1(1400)$ mixing angle is found to be about $51°$. The sign of the mixing angle is fixed by the observed relative strength of $B \to K_1(1270)\gamma$ and $K_1(1400)\gamma$. The formalism is then applied to $B_s \to M$ tensor form factors. We find that the calculated $B_s \to \phi\gamma$ rate is consistent with experiment, though in the lower end of the data. The branching fractions of $B_s \to f_1(1420)\gamma$ and $f_2'(1525)\gamma$ are predicted to be of order 10^{-5} and it will be interesting to search for these modes. Rates on $B_s \to f_1(1285)\gamma$, $h_1(1380)\gamma$, $h_1(1170)\gamma$, $f_2(1270)\gamma$ decays are also predicted.

DOI: 10.1103/PhysRevD.81.114006 PACS numbers: 13.20.He, 13.40.Hq

I. INTRODUCTION

In this work we shall investigate the $B \to M$ tensor form factors and their implications on the exclusive radiative $B_{(s)} \to M\gamma$ decays for $\Delta S = 1$ transitions with M denoting a vector meson V, an axial-vector meson A, or a tensor meson T. These decays receive the dominant contributions from the short-distance electromagnetic penguin process $b \to s\gamma$. These modes are of great interest since they are loop-induced processes and are, hence, sensitive to new physics contributions. Recently, both CDF [1] and D0 [2] have observed 1-2σ deviations from the standard model prediction for the $B_s - \bar{B}_s$ mixing angle. It will be useful to the search for new physics in the $B_{u,d,s}$ systems in the forthcoming experiments at Fermilab, LHCb, and Super B factories.

The radiative decay $B \to K^*\gamma$ was first measured by CLEO [3] and subsequently updated by CLEO [4], *BABAR* [5], and Belle [6] with the result

$$\begin{aligned}
&\mathcal{B}(B^0 \to K^{*0}\gamma) \\
&\quad = \begin{cases} (4.55 \pm 0.70 \pm 0.34) \times 10^{-5} & \text{CLEO} \\ (4.47 \pm 0.10 \pm 0.16) \times 10^{-5} & \textit{BABAR} \\ (4.01 \pm 0.21 \pm 0.17) \times 10^{-5} & \text{Belle,} \end{cases} \\
&\mathcal{B}(B^+ \to K^{*+}\gamma) \\
&\quad = \begin{cases} (3.76 \pm 0.86 \pm 0.28) \times 10^{-5} & \text{CLEO} \\ (4.22 \pm 0.14 \pm 0.16) \times 10^{-5} & \textit{BABAR} \\ (4.25 \pm 0.31 \pm 0.24) \times 10^{-5} & \text{Belle.} \end{cases}
\end{aligned} \tag{1.1}$$

The average branching fractions are [7]

$$\begin{aligned}
\mathcal{B}(B^0 \to K^{*0}\gamma) &= (4.33 \pm 0.15) \times 10^{-5}, \\
\mathcal{B}(B^+ \to K^{*+}\gamma) &= (4.21 \pm 0.18) \times 10^{-5}.
\end{aligned} \tag{1.2}$$

While the decay $B^- \to K_1(1270)^-\gamma$ has been observed by Belle in 2004, other $B \to K_1\gamma$ decays have not been seen and only upper limits were reported [8]:

$$\begin{aligned}
\mathcal{B}(B^- \to K_1^-(1270)\gamma) &= (4.3 \pm 0.9 \pm 0.9) \times 10^{-5}, \\
\mathcal{B}(B^- \to K_1^-(1400)\gamma) &< 1.5 \times 10^{-5}, \\
\mathcal{B}(B^0 \to K_1^0(1270)\gamma) &< 5.8 \times 10^{-5}, \\
\mathcal{B}(B^0 \to K_1^0(1400)\gamma) &< 1.2 \times 10^{-5}.
\end{aligned} \tag{1.3}$$

As for the decay $B \to K_2^*(1430)\gamma$, CLEO [4] has reported the first evidence with the combined result of neutral and charged B modes

$$\mathcal{B}(B \to K_2^*\gamma) = (1.66^{+0.59}_{-0.53} \pm 0.13) \times 10^{-5}. \tag{1.4}$$

Later, the Belle measurement [9] yielded

$$\mathcal{B}(B^0 \to K_2^{*0}\gamma) = (1.3 \pm 0.5 \pm 0.1) \times 10^{-5}, \tag{1.5}$$

while *BABAR* [10] obtained

$$\begin{aligned}
\mathcal{B}(B^0 \to K_2^{*0}\gamma) &= (1.22 \pm 0.25 \pm 0.10) \times 10^{-5}, \\
\mathcal{B}(B^+ \to K_2^{*+}\gamma) &= (1.45 \pm 0.40 \pm 0.15) \times 10^{-5}.
\end{aligned} \tag{1.6}$$

For radiative B_s decays, Belle has reported the first obser-

vation of $B_s \to \phi\gamma$ decay [11] with the result

$$\mathcal{B}(B_s \to \phi\gamma) = (5.7^{+1.8+1.2}_{-1.5-1.1}) \times 10^{-5}. \quad (1.7)$$

This is the only radiative B_s decay that has been observed so far. Its rate is similar to those in $B_{u,d} \to K^*\gamma$ decays. Given the fact that $\tau(B_s) < \tau(B_{u,d})$ [12], one will naively expect a slightly smaller rate for $B_s \to \phi\gamma$.

Using the light-cone sum rule (LCSR) result of 0.38 ± 0.06 [13] for the form factor $T_1(0)$ to be defined below and the $B \to K^*\gamma$ decay amplitude with nonfactorizable corrections evaluated in the QCD factorization (QCDF) approach [14], it was found in [15,16] that the next-to-leading-order (NLO) corrections will enhance the $B \to K^*\gamma$ rate to the extent that its branching fraction disagrees with the observed one (1.2).

In our previous work [17], various $B \to M$ tensor form factors were calculated within the framework of the covariant light-front (CLF) approach [18,19]. This formalism preserves the Lorentz covariance in the light-front framework and has been applied successfully to describe various properties of pseudoscalar and vector mesons [18]. We extended the analysis of the covariant light-front model to even-parity, p-wave mesons [19]. Recently, the CLF approach has been further extended to the studies of the quarkonium system, the B_c system and so on (see, for example, [20]).

We have pointed out in [19] that relativistic effects could manifest in heavy-to-light transitions at maximum recoil where the final-state meson can be highly relativistic and hence there is no reason to expect that the nonrelativistic quark model is still applicable there. Hence, we believe that the CLF approach can provide useful information on $B \to M$ transitions at maximum recoil, the kinematic region relevant to $B \to M\gamma$ decays, and may shed new light on the above-mentioned puzzle.

In [17], we showed that a form factor $T_1(0)$ substantially smaller than what expected from LCSR was obtained, and a significantly improved agreement with experiment was achieved with the rate calculated using the QCDF method. Since we have studied p-wave mesons before in the CLF approach [19], the extension to $B \to K_{1,2}$ transitions, which could be very difficult for lattice QCD calculations, was performed straightforwardly and rates on $B \to K_{1,2}\gamma$ decays were predicted using the calculated form factors as inputs [17].

In the present work, we revise and extend the analysis of [17]. We improve the estimation of the K_{1A} and K_{1B} mixing angle, where K_{1A} and K_{1B} are the $^3P_1$ and $^1P_1$ states of K_1, respectively, and are related to the physical $K_1(1270)$ and $K_1(1400)$ states. As will be shown later, the analysis is done consistently within the covariant light-front approach. After obtaining tensor form factors in the CLF approach, we use QCDF as the main theoretical framework to calculate branching fractions of $B \to K^*\gamma$, $K_1\gamma$, and $K_2\gamma$ decays. We further extend our study to radiative decays $B_s \to \phi\gamma$, $f_1(1420)\gamma$, $f_1(1285)\gamma$, $h_1(1380)\gamma$, $h_1(1170)\gamma$, $f_2'(1525)\gamma$, and $f_2(1270)\gamma$. The calculated $B_s \to \phi\gamma$ rate is in agreement with data. Predictions on the decay rates of other modes are made and can be checked in future experiments.

The paper is organized as follows. The analytic expressions of the tensor form factors evaluated in the covariant light-front model are recollected in Sec. II for completeness. The numerical results for form factors and decay rates together with discussions are shown in Sec. III. The conclusion is given in Sec. IV. The formalism and calculation of the tensor form factors in the covariant light-front model are shown in Appendix A, while input parameters for radiative B decay amplitudes in the QCDF approach are collected in Appendix B.

II. TENSOR FORM FACTORS

The matrix element for the $B_q \to M\gamma$ transition with $M = V, A, T$ mesons is given by

$$iM = \langle \bar{M}(P'', \varepsilon'')\gamma(q, \varepsilon)| - iH_{\rm eff}|\bar{B}_q(P')\rangle, \quad (2.1)$$

where

$$H_{\rm eff} = -\frac{G_F}{\sqrt{2}} V_{ts}^* V_{tb} c_7^{\rm eff} Q_7,$$
$$Q_7 = \frac{e}{8\pi^2} m_b \bar{s}\sigma_{\mu\nu}(1+\gamma_5) b F^{\mu\nu}, \quad (2.2)$$

with $P^{\prime(\prime\prime)}$ being the incoming (outgoing) momentum, $\varepsilon^{(\prime\prime)}$ the polarization vector of γ (M), V_{ij} the corresponding Cabbibo-Kobayashi-Maskawa (CKM) matrix element, and $c_7^{\rm eff}$ the effective Wilson coefficient. By replacing $c_7^{\rm eff}$ by the effective parameter a_7, to be discussed below in Sec. III, nonfactorizable corrections to the $B_q \to M\gamma$ amplitude are included. In this work we will update the calculation of the $B \to K^*$ and $B \to K_1$, K_2^* transition tensor form factors in the covariant light-front quark model and extend the study to $B_s \to M\gamma$ decays.

Tensor form factors for $B_q \to V, A, T$ transitions are defined by

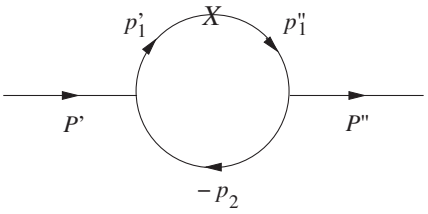

FIG. 1. Feynman diagrams for meson transition amplitudes, where $P^{\prime(\prime\prime)}$ is the incoming (outgoing) meson momentum, $p_1^{\prime(\prime\prime)}$ is the quark momentum, p_2 is the antiquark momentum, and X denotes the corresponding $\bar{q}''\sigma_{\mu\nu}(1+\gamma_5)q'$ transition vertex.

$$\begin{aligned}
\langle \bar{V}(P'', \varepsilon'')|\bar{s}\sigma_{\mu\nu}q^\nu(1+\gamma_5)b|\bar{B}_q(P')\rangle &= i\epsilon_{\mu\nu\lambda\rho}\varepsilon''^{\nu*}P^\lambda q^\rho T_1(q^2) + (\varepsilon''^*_\mu P\cdot q - P_\mu \varepsilon''^*\cdot q)T_2(q^2) \\
&\quad + \varepsilon''^*\cdot q\left(q_\mu - P_\mu\frac{q^2}{P\cdot q}\right)T_3(q^2), \\
\langle A_{^3P_1,{}^1P_1}(P'', \varepsilon'')|\bar{s}\sigma_{\mu\nu}q^\nu(1+\gamma_5)b|\bar{B}_q(P')\rangle &= i\epsilon_{\mu\nu\lambda\rho}\varepsilon''^{\nu*}P^\lambda q^\rho Y_{A1,B1}(q^2) + (\varepsilon''^*_\mu P\cdot q - P_\mu \varepsilon''^*\cdot q)Y_{A2,B2}(q^2) \\
&\quad + \varepsilon''^*\cdot q\left(q_\mu - P_\mu\frac{q^2}{P\cdot q}\right)Y_{A3,B3}(q^2), \\
\langle T(P'', \varepsilon'')|\bar{s}\sigma_{\mu\nu}q^\nu(1+\gamma_5)b|\bar{B}_q(P')\rangle &= -i\epsilon_{\mu\nu\lambda\rho}\varepsilon''^{\nu\sigma*}P_\sigma P^\lambda q^\rho\frac{U_1(q^2)}{m_{B_q}} - (\varepsilon''^*_{\mu\sigma}P\cdot q - P_\mu\varepsilon''^*_{\sigma\rho}q^\rho)P^\sigma\frac{U_2(q^2)}{m_{B_q}} \\
&\quad - \varepsilon''^*_{\sigma\rho}P^\sigma q^\rho\left(q_\mu - P_\mu\frac{q^2}{P\cdot q}\right)\frac{U_3(q^2)}{m_{B_q}},
\end{aligned} \tag{2.3}$$

where $P = P' + P''$, $q = P' - P''$ and the convention $\epsilon^{0123} = +1$ is adopted.

A brief derivation of $B_q \to V, A, T$ transition tensor form factors from the diagram depicted in Fig. 1 is shown in Appendix A. Here, only the final analytic results are given. First of all, the $B_q \to V$ transition form factors are given by [17]

$$\begin{aligned}
T_1(q^2) &= \frac{N_c}{16\pi^3}\int dx_2 d^2p'_\perp \frac{h'_P h''_V}{x_2\hat{N}'_1\hat{N}''_1}\Big\{2A_1^{(1)}[M'^2 - M''^2 - 2m_1'^2 - 2\hat{N}'_1 + q^2 + 2(m'_1m_2 + m''_1m_2 - m'_1m''_1)] \\
&\quad - 8A_1^{(2)} + (m'_1 + m''_1)^2 + \hat{N}'_1 + \hat{N}''_1 - q^2 + 4(M'^2 - M''^2)(A_2^{(2)} - A_3^{(2)}) + 4q^2(-A_1^{(1)} + A_2^{(1)} + A_3^{(2)} - A_4^{(2)}) \\
&\quad - \frac{4}{w''_V}[(m'_1 + m''_1)A_1^{(2)}]\Big\}, \\
T_2(q^2) &= T_1(q^2) + \frac{q^2}{(M'^2 - M''^2)}\frac{N_c}{16\pi^3}\int dx_2 d^2p'_\perp \frac{h'_P h''_V}{x_2\hat{N}'_1\hat{N}''_1}\Big\{2A_2^{(1)}[M'^2 - M''^2 - 2m_1'^2 - 2\hat{N}'_1 + q^2 \\
&\quad + 2(m'_1m_2 + m''_1m_2 - m'_1m''_1)] - 8A_1^{(2)} - 2M'^2 + 2m_1'^2 + (m'_1 + m''_1)^2 + 2(m_2 - 2m'_1)m_2 + 3\hat{N}'_1 + \hat{N}''_1 - q^2 \\
&\quad + 2Z_2 + 4(q^2 - 2M'^2 - 2M''^2)(A_2^{(2)} - A_3^{(2)}) - 4(M'^2 - M''^2)(-A_1^{(1)} + A_2^{(1)} + A_3^{(2)} - A_4^{(2)}) \\
&\quad - \frac{4}{w''_V}[(m''_1 - m'_1 + 2m_2)A_1^{(2)}]\Big\}, \\
T_3(q^2) &= \frac{N_c}{16\pi^3}\int dx_2 d^2p'_\perp \frac{h'_P h''_V}{x_2\hat{N}'_1\hat{N}''_1}\Big\{-2A_2^{(1)}[M'^2 - M''^2 - 2m_1'^2 - 2\hat{N}'_1 + q^2 + 2(m'_1m_2 + m''_1m_2 - m'_1m''_1)] \\
&\quad + 8A_1^{(2)} + 2M'^2 - 2m_1'^2 - (m'_1 + m''_1)^2 - 2(m_2 - 2m'_1)m_2 - 3\hat{N}'_1 - \hat{N}''_1 + q^2 - 2Z_2 - 4(q^2 - M'^2 - 3M''^2) \\
&\quad \times (A_2^{(2)} - A_3^{(2)}) + \frac{4}{w''_V}\{(m''_1 - m'_1 + 2m_2)[A_1^{(2)} + (M'^2 - M''^2)(A_2^{(2)} + A_3^{(2)} - A_1^{(1)})] \\
&\quad + (m'_1 + m''_1)(M'^2 - M''^2)(A_2^{(1)} - A_3^{(2)} - A_4^{(2)}) + m'_1(M'^2 - M''^2)(A_1^{(1)} + A_2^{(1)} - 1)\}\Big\}.
\end{aligned} \tag{2.4}$$

The expressions of h', h'', $\hat{N}'$, $\hat{N}''$, $A_j^{(i)}$, and Z_2 can be found in the Appendix A.

Second, the $B_q \to A$ transition form factors can be obtained from the above expressions by applying a simple relation [17] (see also Appendix A):

$$Y_{Ai,Bi}(q^2) = T_i(q^2) \quad \text{with} \quad (m''_1 \to -m''_1, h''_V \to h''_{^3A,{}^1A}, w''_V \to w''_{^3A,{}^1A}), \tag{2.5}$$

for $i = 1, 2, 3$. Note that only the $1/w''$ terms in Y_{Bi} form factors are kept, and we should be cautious that the replacement of $m''_1 \to -m''_1$ should not be applied to m''_1 in w'' and h''.

Third, the $B_q \to T$ transition form factors are given by [17]

$$
\begin{aligned}
U_1(q^2) &= \frac{N_c}{16\pi^3}\int dx_2 d^2p'_\perp \frac{M' h'_P h''_T}{x_2 \hat{N}'_1 \hat{N}''_1}\Big\{2(A_1^{(1)}-A_2^{(2)}-A_3^{(2)})[M'^2-M''^2-2m_1'^2-2\hat{N}'_1+q^2+2(m'_1m_2+m''_1m_2-m'_1m''_1)] \\
&\quad -8(A_1^{(2)}-A_1^{(3)}-A_2^{(3)})+(1-A_1^{(1)}-A_2^{(1)})[(m'_1+m''_1)^2+\hat{N}'_1+\hat{N}''_1-q^2]+4(M'^2-M''^2) \\
&\quad \times(A_2^{(2)}-A_3^{(2)}-A_3^{(3)}+A_5^{(3)})+4q^2(-A_1^{(1)}+A_2^{(1)}+A_2^{(2)}+A_3^{(2)}-2A_4^{(2)}-A_4^{(3)}+A_6^{(3)})-2(A_1^{(2)}+2A_1^{(3)}-2A_2^{(3)}) \\
&\quad -\frac{8}{w''_V}[(m'_1+m''_1)(A_1^{(2)}-A_1^{(3)}-A_2^{(3)})]\Big\}, \\
U_2(q^2) &= U_1(q^2)+\frac{q^2}{(M'^2-M''^2)}\frac{N_c}{16\pi^3}\int dx_2 d^2p'_\perp \frac{M' h'_P h''_T}{x_2 \hat{N}'_1 \hat{N}''_1}\Big\{2(A_2^{(1)}-A_3^{(2)}-A_4^{(2)})[M'^2-M''^2-2m_1'^2-2\hat{N}'_1+q^2 \\
&\quad +2(m'_1m_2+m''_1m_2-m'_1m''_1)]-8(A_1^{(2)}-A_1^{(3)}-A_2^{(3)})+(1-A_1^{(1)}-A_2^{(1)})[-2M'^2+2m_1'^2+(m'_1+m''_1)^2 \\
&\quad +2(m_2-2m'_1)m_2+3\hat{N}'_1+\hat{N}''_1-q^2]+2\Big[Z_2(1-A_2^{(1)})-\frac{P\cdot q}{q^2}A_1^{(2)}\Big]+4(q^2-2M'^2-2M''^2) \\
&\quad \times(A_2^{(2)}-A_3^{(2)}-A_3^{(3)}+A_5^{(3)})-4(M'^2-M''^2)(-A_1^{(1)}+A_2^{(1)}+A_2^{(2)}+A_3^{(2)}-2A_4^{(2)}-A_4^{(3)}+A_6^{(3)}) \\
&\quad +2(A_1^{(2)}+2A_1^{(3)}-2A_2^{(3)})-\frac{8}{w''_V}[(m''_1-m'_1+2m_2)(A_1^{(2)}-A_1^{(3)}-A_2^{(3)})]\Big\}, \\
U_3(q^2) &= \frac{N_c}{16\pi^3}\int dx_2 d^2p'_\perp \frac{M' h'_P h''_T}{x_2 \hat{N}'_1 \hat{N}''_1}\Big\{-2(A_2^{(1)}-A_3^{(2)}-A_4^{(2)})[M'^2-M''^2-2m_1'^2-2\hat{N}'_1+q^2+2(m'_1m_2+m''_1m_2-m'_1m''_1)] \\
&\quad +8(A_1^{(2)}-A_1^{(3)}-A_2^{(3)})-(1-A_1^{(1)}-A_2^{(1)})[-2M'^2+2m_1'^2+(m'_1+m''_1)^2+2(m_2-2m'_1)m_2+3\hat{N}'_1+\hat{N}''_1-q^2] \\
&\quad -2\Big[Z_2(1-A_2^{(1)})-\frac{P\cdot q}{q^2}A_1^{(2)}\Big]-4(q^2-M'^2-3M''^2)(A_2^{(2)}-A_3^{(2)}-A_3^{(3)}+A_5^{(3)})-2(A_1^{(2)}+2A_1^{(3)}-2A_2^{(3)}) \\
&\quad +\frac{4}{w''_V}\{(m''_1-m'_1+2m_2)[2(A_1^{(2)}-A_1^{(3)}-A_2^{(3)})+(M'^2-M''^2)(-A_1^{(1)}+2A_2^{(2)}+2A_3^{(2)}-A_3^{(3)}-2A_4^{(3)}-A_5^{(3)})] \\
&\quad +(m'_1+m''_1)(M'^2-M''^2)(A_2^{(1)}-2A_3^{(2)}-2A_4^{(2)}+A_4^{(3)}+2A_5^{(3)}+A_6^{(3)}) \\
&\quad +m'_1(M'^2-M''^2)(-1+2A_1^{(1)}+2A_2^{(1)}-A_2^{(2)}-2A_3^{(2)}-A_4^{(2)})\}\Big\}. \qquad (2.6)
\end{aligned}
$$

We are now ready to calculate the radiative decay rates. Before proceeding, several remarks are in order: (i) At $q^2=0$, the form factors obey the simple relations: $T_2(0)=T_1(0)$, $Y_{A2,B2}(0)=Y_{A1,B1}(0)$, and $U_2(0)=U_1(0)$. (ii) Form factors $T_3(0)$, $Y_{A3,B3}(0)$, $U_3(0)$ do not contribute to the $B\to M\gamma$ radiative decay rates. (iii) There are some new terms in the above form factor expressions that were missed in [17]. As we shall see in the next section, the resulting $B\to M\gamma$ rates are modified sizably for some modes. It is straightforward to obtain [17][1]

$$
\begin{aligned}
\mathcal{B}(B_q\to V\gamma) &= \tau_{B_q}\frac{G_F^2\alpha m_{B_q}^3 m_b^2}{32\pi^4}\Big(1-\frac{m_V^2}{m_{B_q}^2}\Big)^3|V_{cb}V_{cs}^* a_7^c T_1(0)|^2, \\
\mathcal{B}(B_q\to A_{^3P_1,^1P_1}\gamma) &= \tau_{B_q}\frac{G_F^2\alpha m_{B_q}^3 m_b^2}{32\pi^4}\Big(1-\frac{m_{A_{^3P_1,^1P_1}}^2}{m_{B_q}^2}\Big)^3|V_{cb}V_{cs}^* a_7^c Y_{A1,B1}(0)|^2, \qquad (2.7) \\
\mathcal{B}(B_q\to T\gamma) &= \tau_{B_q}\frac{G_F^2\alpha m_{B_q}^5 m_b^2}{256\pi^4 m_T^2}\Big(1-\frac{m_T^2}{m_{B_q}^2}\Big)^5|V_{cb}V_{cs}^* a_7^c U_1(0)|^2,
\end{aligned}
$$

where τ_{B_q} is the lifetime of the B_q meson and m_b is the $\overline{\rm MS}$ b-quark mass. The effective Wilson coefficient $a_7(V\gamma)$ [15,16,21] and $a_7(A\gamma)$ [22] are calculated in the QCDF approach [14]. They consist of several different contributions [15,16,21,22]:

$$
a_7^c(\mu)=c_7^{\rm eff}(\mu)+a_{7,\rm ver}^c(\mu)+a_{7,\rm sp}^c(\mu_h), \qquad (2.8)
$$

[1]Since $|V_{cb}V_{cs}^*|\gg|V_{ub}V_{us}^*|$, for the purpose of obtaining the radiative decay rates, we only consider the $|V_{cb}V_{cs}^* a_7^c|^2$ contributions.

where $c_7^{\rm eff}$, $a_{7,\rm ver}$, and $a_{7,\rm sp}$ are the NLO Wilson coefficient, the vertex, and hard-spectator corrections, respectively. The last two terms in the above equation are given by

$$a^c_{7,\rm ver}(\mu) = \frac{\alpha_s(\mu)C_F}{4\pi}[c_1(\mu)G_1(m_c^2/m_b^2) + c_8^{\rm eff}(\mu)G_8],$$
$$a^c_{7,\rm sp}(\mu_h) = \frac{\alpha_s(\mu_h)C_F}{4\pi}[c_1(\mu_h)H_1(m_c^2/m_b^2) + c_8^{\rm eff}(\mu_h)H_8] \tag{2.9}$$

with the hadronic scale $\mu_h \sim \sqrt{\Lambda_h \mu}$ for $\Lambda_h \simeq 0.5$ GeV and $G_{1,8}$, $H_{1,8}$ given in [16]. Note that the analytic expression for $a_7(V\gamma)$ and $a_7(A\gamma)$ are identical, but numerically, due to differences of the wave functions of V and A, $a_{\rm sp}(V\gamma)$ and $a_{\rm sp}(A\gamma)$ could be quite different [22]. As the QCDF calculation of $a_7(T\gamma)$ is not available yet, we shall take

$$a_7^c(T\gamma) \simeq c_7^{\rm eff}(\mu) \tag{2.10}$$

and neglect $a^c_{7,\rm ver}(T\gamma)$ and $a^c_{7,\rm sp}(T\gamma)$ in this work.

In the next section, we will give numerical results for form factors $T_i(q^2)$, $Y_{Ai,Bi}(q^2)$, $U_i(q^2)$, and the corresponding $B_q \to V\gamma$, $A\gamma$, $T\gamma$ decay rates.

III. NUMERICAL RESULTS AND DISCUSSION

A. $B \to M$ tensor form factors and $B \to K^*\gamma$, $K_1\gamma$, and $K_2^*\gamma$ decays

To perform numerical calculations, first we need to specific some input parameters in the covariant light-front model. The input parameters m_q and β in the Gaussian-type wave function (A11) are shown in Table I. The constituent quark masses are close to those used in the literature [17–19,23–26]. Meson masses and decay widths are taken from [12] and CKM parameters from [27].

The physical K_1 states $K_1(1270)$ and $K_1(1400)$ are mixed states of the K_{1A} and K_{1B} states,

$$K_1(1270) = K_{1A}\sin\theta_{K_1} + K_{1B}\cos\theta_{K_1},$$
$$K_1(1400) = K_{1A}\cos\theta_{K_1} - K_{1B}\sin\theta_{K_1}. \tag{3.1}$$

Since they are not charge conjugation eigenstates, mixing is not prohibited. Indeed, the mixing is governed by the mass difference of the strange and nonstrange light quarks. It follows that the masses of K_{1A} and K_{1B} can be expressed as

$$m^2_{K_{1A}} = m^2_{K_1(1400)}\cos^2\theta_{K_1} + m^2_{K_1(1270)}\sin^2\theta_{K_1},$$
$$m^2_{K_{1B}} = m^2_{K_1(1400)}\sin^2\theta_{K_1} + m^2_{K_1(1270)}\cos^2\theta_{K_1}. \tag{3.2}$$

Note that we need to know the mixing angle θ_{K_1} in order to specify the mass parameters $m_{K_{1A,1B}}$, which in turn will be needed to obtain the numerical results for tensor form factors $Y_{A,B}(q^2)$.

The input parameters β's are fixed by the decay constants whose analytic expressions in the covariant light-front model are given in [19]. We use $f_B = 200 \pm 15$ MeV, $f_{B_s} = 240 \pm 15$ MeV, $f_{K^*} = 220$ MeV, and $f_\phi = 230$ MeV to fix β's. For p-wave strange mesons, we take for simplicity $\beta_{K_1} = \beta_{K_{1A}} = \beta_{K_{1B}} = \beta_{K_2^*}$ [28]. To fix β_{K_1}, we need the information of the $K_1(1270)$ and $K_1(1400)$ decay constants.

There exist several estimations on the mixing angle θ_{K_1} in the literature. From the early experimental information on masses and the partial rates of $K_1(1270)$ and $K_1(1400)$, Suzuki found two possible solutions with a two-fold ambiguity, $|\theta_{K_1}| \approx 33^\circ$ and 57° [29]. A similar constraint $35^\circ \lesssim |\theta_{K_1}| \lesssim 55^\circ$ was obtained in [30] based solely on two parameters: the mass difference of the a_1 and b_1 mesons and the ratio of the constituent quark masses. An analysis of $\tau \to K_1(1270)\nu_\tau$ and $K_1(1400)\nu_\tau$ decays also yielded the mixing angle to be $\approx 37^\circ$ or 58° with a two-fold ambiguity [31]. Most of these estimations were obtained by assuming a vanishing $f_{K_{1B}}$. With the help of analytical expressions for $f_{K_{1A,1B}}$ obtained in the CLF quark model [19], we can now release this assumption. Using the experimental results $\mathcal{B}(\tau \to K_1(1270)\nu_\tau) = (4.7 \pm 1.1) \times 10^{-3}$ and $\Gamma(\tau \to K_1(1270)\nu_\tau)/[\Gamma(\tau \to K_1(1270)\nu_\tau) + \Gamma(\tau \to K_1(1400)\nu_\tau)] = 0.69 \pm 0.15$ [12], we obtain[2]

$$|f_{K_1(1400)}| = 139.2^{+41.3}_{-45.6}\ \text{MeV},$$
$$|f_{K_1(1270)}| = 169.5^{+18.8}_{-21.2}\ \text{MeV}. \tag{3.3}$$

These decay constants are related to $f_{K_{1A}}$ and $f_{K_{1B}}$ through

$$m_{K_1(1270)}f_{K_1(1270)} = m_{K_{1A}}f_{K_{1A}}\sin\theta_{K_1} + m_{K_{1B}}f_{K_{1B}}\cos\theta_{K_1},$$
$$m_{K_1(1400)}f_{K_1(1400)} = m_{K_{1A}}f_{K_{1A}}\cos\theta_{K_1} - m_{K_{1B}}f_{K_{1B}}\sin\theta_{K_1}, \tag{3.4}$$

where uses of Eq. (3.1) and equations for decay constants $\langle 0|A_\mu|K_{1A}\rangle = m_{K_{1A}}f_{K_{1A}}\varepsilon_\mu$, $\langle 0|A_\mu|K_1(1270)\rangle = m_{K_1(1270)} \times f_{K_1(1270)}\varepsilon_\mu$ and similar ones for K_{1B} and $K_1(1400)$ have been made. From the analytic expressions of decay constants given in [19], we see that $m_{K_{1A}}f_{K_{1A}}$ and $m_{K_{1B}}f_{K_{1B}}$ are functions of β_{K_1} and quark masses only [see Eqs. (2.23) and (2.11) of [19]]. In other words, they do not depend on $m_{K_{1A,1B}}$ and hence θ_{K_1}. Equation (3.4) leads to the relation

$$m^2_{K_1(1270)}f^2_{K_1(1270)} + m^2_{K_1(1400)}f^2_{K_1(1400)} = m^2_{K_{1A}}f^2_{K_{1A}} + m^2_{K_{1B}}f^2_{K_{1B}}. \tag{3.5}$$

This relation is independent of θ_{K_1}. In practice, we shall use this equation to fix the central value of the parameter β_{K_1} to be 0.3224 GeV.

[2]The large experimental error with the $K_1(1400)$ production in the τ decay, namely, $\mathcal{B}(\tau^- \to K_1^-(1400)\nu_\tau) = (1.7 \pm 2.6) \times 10^{-3}$ [12], does not provide sensible information for the $K_1(1400)$ decay constant.

TABLE I. The input parameters m_q and β (in units of GeV) in the Gaussian-type wave function (A11). The parameter β for f_1, h_1, f_2 is defined for their $s\bar{s}$ component.

m_u	m_s	m_b	β_B	β_{K^*}	β_{K_1,K_2^*}
0.25	0.35	4.45	$0.5671^{+0.0352}_{-0.0354}$	0.2829	$0.3224^{+0.0163}_{-0.0195}$
β_{B_s}	β_ϕ	β_{f_1,h_1,f_2}			
0.6396 ± 0.0566	0.3051	0.3446 ± 0.0064			

Note that in the CLF quark model the signs of the decay constants $f_{K_{1A}}$ and $f_{K_{1B}}$ and their relative signs with respect to form factors are fixed [19].[3] Specifically, we learn from Eq. (2.23) of [19] that $f_{K_{1A}}$ is negative; whereas, $f_{K_{1B}}$ is positive. With this sign convention, we are ready to determine the mixing angle θ_{K_1} from Eq. (3.4). We find two best fit solutions for θ_{K_1}:

$$\theta_{K_1} = \begin{cases} 50.8^\circ & \text{solution I,} \\ -44.8^\circ & \text{solution II.} \end{cases} \tag{3.6}$$

In both cases,

$$\begin{aligned} m_{K_{1A}} f_{K_{1A}} &= -0.2905 \text{ GeV}^2, \\ m_{K_{1B}} f_{K_{1B}} &= 0.0152 \text{ GeV}^2 \end{aligned} \tag{3.7}$$

are obtained. The uncertainty in β_{K_1} for these two mixing angles can be obtained using Eqs. (3.3) and (3.4). The reader may wonder why we do not have a two-fold ambiguity for θ_{K_1}. This is because we do not assume a vanishing $f_{K_{1B}}$, and we demand that $|\theta_{K_1}| \le \pi/2$. From Eq. (3.4), we have

$$\begin{aligned} \theta_{K_1} &= \pm\tan^{-1}\left|\frac{m_{K_1(1270)} f_{K_1(1270)}}{m_{K_1(1400)} f_{K_1(1400)}}\right| + \tan^{-1}\left|\frac{m_{K_{1B}} f_{K_{1B}}}{m_{K_{1A}} f_{K_{1A}}}\right| \\ &= \pm 47.8^\circ + 3.0^\circ. \end{aligned} \tag{3.8}$$

This leads to the above two solutions. Note that in the SU(3) limit, $f_{K_{1B}} = 0$ and $f_{K_1(1270)}/f_{K_1(1400)} = \tan\theta_{K_1}$. As we shall see below, the second solution $\theta_{K_1} = -44.8^\circ$ is ruled out by the experimental measurements of $B \to K_1(1270)\gamma$ and $B \to K_1(1400)\gamma$. For $\theta_{K_1} = 50.8^\circ$, we find

$$\begin{aligned} m_{K_{1A}} &= 1.37 \text{ GeV}, & f_{K_{1A}} &= -212 \text{ MeV}, \\ m_{K_{1B}} &= 1.31 \text{ GeV}, & f_{K_{1B}} &= 12 \text{ MeV}. \end{aligned} \tag{3.9}$$

Since we have imposed the constraint $q^+ = 0$ in the calculation, form factors are obtained only for spacelike momentum transfer $q^2 = -q_\perp^2 \le 0$; whereas, only the timelike form factors are relevant for the physical decay processes. Here, we follow [17,19,23] to take the form factors as explicit functions of q^2 in the spacelike region and then analytically continue them to the timelike region. We find that, except for the form factors Y_{B3} and $U_{2,3}$, the momentum dependence of the form factors T_i, $Y_{Ai,Bi}$, U_i in the spacelike region can be well parametrized and reproduced in the 3 parameter form:

$$F(q^2) = \frac{F(0)}{1 - a(q^2/m_B^2) + b(q^2/m_B^2)^2}. \tag{3.10}$$

We then employ this parametrization to determine the physical form factors at $q^2 \ge 0$. In practice, the parameters a, b, and $F(0)$ are obtained by performing a 3 parameter fit to the form factors in the range $-20 \text{ GeV}^2 \le q^2 \le 0$. The obtained a and b coefficients are in most cases not far from unity as expected. However, the coefficient b for Y_{B3} and $U_{2,3}$ is rather sensitive to the chosen range for q^2 and can be far away from unity. To overcome this difficulty, we fit $Y_{B3}(q^2)$ and $U_3(q^2)$ to the form

$$F(q^2) = F(0)(1 + a(q^2/m_B^2) + b(q^2/m_B^2)^2), \tag{3.11}$$

while for $U_2(q^2)$, we first define $U_2'(q^2)$ through

$$U_2(q^2) = U_1(q^2) + \frac{q^2}{m_B^2} U_2'(q^2), \tag{3.12}$$

and then fit $U_2'(q^2)$ using Eq. (3.10). Note that a decomposition of U_2 into U_1 and U_2' is motivated by Eq. (2.6). The above procedure accomplishes substantial improvements.

The tensor form factors and their q^2 dependence for $B \to K^*$, K_1, K_2^* transitions are shown in Table II and depicted in Fig. 2. Our form factor $T_1(0) = 0.29$ is significantly smaller than the old LCSR result of 0.38 ± 0.06 [13]. A new LCSR calculation yields $0.25^{+0.03}_{-0.02}$ [22], which is close to the lattice result $T_1(0) = 0.24 \pm 0.03^{+0.04}_{-0.01}$ [35]. For the form factors Y_{A1} and Y_{B1} (or sometimes called $T_1^{K_{1A}}$ and $T_1^{K_{1B}}$, respectively, in the literature), we compare our results with other model calculations in Table III. It is clear

[3]The relative signs of the decay constants, form factors, and mixing angles of the axial-vector mesons were often very confusing in the literature. As stressed in [32], the sign of the mixing angle θ_{K_1} is intimately related to the relative sign of the K_{1A} and K_{1B} states. In the light-front quark model [19] and in perturbative QCD (pQCD) [33], the decay constants of K_{1A} and K_{1B} are of opposite signs, while the $D(B) \to K_{1A}$ and $D(B) \to K_{1B}$ form factors are of the same sign. The mixing angle θ_{K_1} is positive. It is the other way around in the approaches of QCD sum rules [34] and the Isgur-Scora-Grinstein-Wise model [28]: the decay constants of K_{1A} and K_{1B} have the same sign, while the $D(B) \to K_{1A}$ and $D(B) \to K_{1B}$ form factors are opposite in sign. These two conventions are related via a redefinition of the K_{1A} or K_{1B} state, i.e., $K_{1A} \to -K_{1A}$ or $K_{1B} \to -K_{1B}$.

TABLE II. Tensor form factors of $B \to K^*, K_1, K_2^*$ transitions obtained in the covariant light-front model are fitted to the 3 parameter form Eq. (3.10) except for Y_{B3} and $U_{2,3}$. Central values of β's listed in Table I are used. All form factors are dimensionless. For $B \to K_{1A,1B}$ transition form factors, only results with $\theta_{K_1} = 50.8°$ are shown since one needs to specify the value of θ_{K_1} in order to fix the values of $m_{K_{1A,1B}}$.

F	$F(0)$	$F(q^2_{\rm max})$	a	b	F	$F(0)$	$F(q^2_{\rm max})$	a	b
T_1	0.29	1.09	1.86	1.16	Y_{A1}	0.36	1.20	1.61	0.64
T_2	0.29	0.91	1.03	0.06	Y_{A2}	0.36	0.58	0.63	−0.11
T_3	0.18	0.54	1.48	0.74	Y_{A3}	0.21	0.30	0.76	0.36
Y_{B1}	0.13	0.35	1.88	1.39	U_1	0.28	0.62	2.27	2.33
Y_{B2}	0.14	0.26	1.00	0.23	U_2[a]	0.28	1.04	...	...
Y_{B3}[b]	−0.05	−0.17	2.65	0.00	U_2'[b]	0.41	0.78	1.87	1.82
					U_3[b]	−0.25	−0.68	−2.27	1.77

[a]We use $U_2 \equiv U_1 + (q^2/m_B^2)U_2'$ and fit for U_2' using Eq. (3.10).
[b]Y_{B3} and U_3 are fitted using Eq. (3.11).

that while the CLF quark model, pQCD [36], and LCSR [22] all lead to a similar Y_{A1}, the predicted Y_{B1} is smaller in the CLF model.

We are now ready to discuss the implications on $B \to M\gamma$ decay rates. The decay $B \to K^*\gamma$ has been considered in [15,16] within the framework of the QCD factorization approach. The results of [15,16,21] are consistent with each other for the same value of the form factor $T_1(0)$. For $a_7^c(V\gamma)$ and $a_7^c(A\gamma)$ we shall use Eqs. (2.8) and (2.9) calculated in QCDF with input parameters collected in Appendix B. For example, using the formulas given in [16,22] and the central values of input parameters, we obtain

$$\begin{aligned} a_7^c(m_b) = {} & -0.3107 + (-0.079 - i0.014) \\ & + \frac{f_B f_M^\perp}{m_B F^{B\to M}(0)\lambda_B}(\mu_h)[(-0.7906 - 0.7643i)a_0^\perp \\ & \times (\mu_h) + (-0.2893 + 0.5024i)a_1^\perp(\mu_h) \\ & + (0.1676 + 0.4252i)a_2^\perp(\mu_h)], \end{aligned} \tag{3.13}$$

where contributions from NLO $c_7^{\rm eff}$, $a_{7,\rm ver}^c$, and $a_{7,\rm sp}^c$ are shown separately and $a_i^\perp$ are Gegenbauer moments of the meson wave function. The value of $a_7(K^*\gamma)$ is substantially larger than the Wilson coefficient $c_7^{\rm eff}$ of order -0.31 at $\mu = m_b$. For the $K_2^*\gamma$ modes, we shall employ $a_7 = c_7^{\rm eff}$ as NLO QCD corrections from vertex and hard-spectator contributions there have not been calculated yet.

In Table IV, we summarize the calculated branching fractions for the radiative decays $B \to K^*\gamma$, $K_1(1270)\gamma$, $K_1(1400)\gamma$, $K_2^*(1430)\gamma$ in the covariant light-front model. The theoretical errors arise from the uncertainties in form factors, a_7, $|V_{cb}V_{cs}^*|$, and m_b (see Appendix B). For comparison, we also quote experimental results and some other theoretical calculations. For results in light front quark model [39], lattice [35], and LCSR [40], we also use Eqs. (2.8) and (2.9). For $B \to K^*\gamma$ rates from the relativistic quark model [38] and heavy quark effective theory (HQET) [42], we have scaled up their results by a factor of $|a_7(K^*\gamma)/c_7^{\rm eff}|^2 = 1.78$. Calculations in LCSR [40] and HQET [42] are often expressed in terms of $R \equiv \mathcal{B}(B \to K^{**}\gamma)/\mathcal{B}(b \to s\gamma)$ with K^{**} denoting K_1 or K_2^*. Therefore, the branching fraction of $B \to K^{**}\gamma$ is obtained by multiplying R with $\mathcal{B}(b \to s\gamma) = 3.52 \times 10^{-4}$ [7]. Results obtained from large energy effective theory [21], QCDF with long-distance contributions [41], soft-collinear effective theory (SCET) [43], and pQCD [44] calculations are also compared.[4]

TABLE III. Tensor form factors $Y_{A1}^{K_{1A}}$ and $Y_{B1}^{K_{1B}}$ at $q^2 = 0$ in various approaches.

Form factor	This work	pQCD [36]	LCSR [22]	LCSR [37]
$Y_{A1}^{K_{1A}}(0)$	0.36 ± 0.02	$0.37^{+0.08}_{-0.07}$	$0.31^{+0.09}_{-0.05}$	...[a]
$Y_{B1}^{K_{1B}}(0)$	0.13 ± 0.01	$0.29^{+0.09}_{-0.09}$	$0.25^{+0.06}_{-0.07}$[b]	$0.256^{+0.0040}_{-0.0044}$

[a]The form factor Y_{A1} was not computed in [37].
[b]In our sign convention for $|K_1(1270)\rangle$ and $|K_{1B}\rangle$ states.

As stressed in [15,16], the NLO correction yields an enhancement of the $B \to K^*\gamma$ rate that can be as large as 80%. Consequently, the predicted rate will become too large if the tensor form factor $T_1(0)$ is larger than 0.30. Our prediction of $\mathcal{B}(B \to K^*\gamma) = (4.28^{+2.78}_{-1.46}) \times 10^{-5}$ due to short-distance $b \to s\gamma$ contributions agrees with experiment (see Table IV).

From Table IV, we see that our updated $K_1(1270)\gamma$ and $K_1(1400)\gamma$ rates for $\theta_{K_1} = 50.8°$ are in good agreement with the data. Evidently, the other mixing angle $\theta_{K_1} = -44.8°$ is ruled out by experiment. As first pointed out in [17], the $K_1(1400)\gamma$ rate is substantially smaller than that of $K_1(1270)\gamma$. This can be seen from the physical form factors

$$\begin{aligned} Y_1^{K_1(1270)} &= Y_{A1}\sin\theta_{K_1} + Y_{B1}\cos\theta_{K_1}, \\ Y_1^{K_1(1400)} &= Y_{A1}\cos\theta_{K_1} - Y_{B1}\sin\theta_{K_1}. \end{aligned} \tag{3.14}$$

It is obvious that the form factor Y_1 is large for $K_1(1270)$ and small for $K_1(1400)$ when $\theta_{K_1} = 50.8°$.

For $B \to K_2^*\gamma$ decays, the calculated branching fraction $(2.94^{+3.18}_{-1.39}) \times 10^{-5}$ agrees with the world average of $(1.45 \pm 0.43) \times 10^{-5}$ within errors. It should be stressed that the above prediction is for $a_7(K_2^*\gamma) \simeq c_7^{\rm eff}$. Therefore, a small but destructive NLO correction will be helpful to improve the discrepancy.

[4]The pQCD results for $B \to K_1(1270)\gamma$ and $K_1(1400)\gamma$ rates in [44] are not displayed in Table IV since the $B \to K_{1A}$ and $B \to K_{1B}$ transition form factors there are erroneous, though they have been corrected in [36].

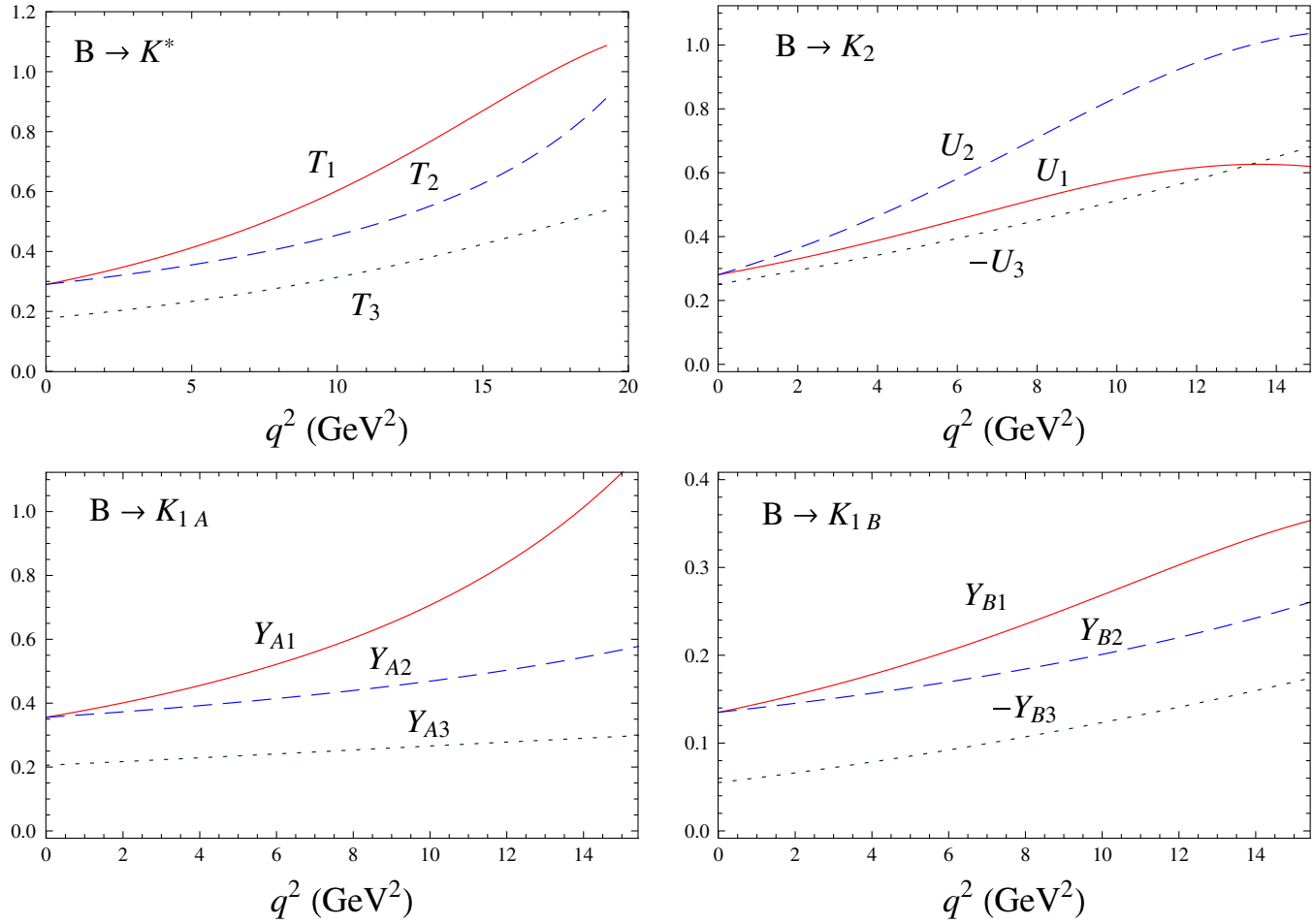

FIG. 2 (color online). Tensor form factors $T_i(q^2)$, $Y_{Ai,Bi}(q^2)$, and $U_i(q^2)$ for $B \to K^*$, $B \to K_1$, and $B \to K_2^*$ transitions, respectively.

B. $B_s \to M$ tensor form factors and $B_s \to \phi\gamma, h_1\gamma, f_1\gamma$, and $f_2\gamma$ decays

We use $f_{B_s} = 240 \pm 15$ MeV and $f_\phi = 230$ MeV to fix the input parameters β_{B_s} and β_ϕ, respectively. For p-wave mesons, there are mixing between singlet and octet states or, equivalently, between $u\bar{u} + d\bar{d}$ and $s\bar{s}$ components, where only the $s\bar{s}$ components are relevant to $B_s \to M\gamma$ transitions. We follow [12] to use

$$\begin{aligned} f' &= \frac{1}{\sqrt{2}}(u\bar{u} + d\bar{d})\cos\alpha - s\bar{s}\sin\alpha, \\ f &= \frac{1}{\sqrt{2}}(u\bar{u} + d\bar{d})\sin\alpha + s\bar{s}\cos\alpha, \end{aligned} \tag{3.15}$$

with $(f', f) = (h_1(1380), h_1(1170))$ for $^1P_1$ states, $(f_1(1420), f_1(1285))$ for $^3P_1$ states, and $(f_2'(1525), f_2(1270))$ for $^3P_2$ tensor states [12]. The mixing angle α is related to the singlet-octet mixing angle θ by the relation $\alpha = \theta + 54.7°$. The latter mixing angle is defined by

$$f' = f_8\cos\theta - f_1\sin\theta, \qquad f = f_8\sin\theta + f_1\cos\theta, \tag{3.16}$$

and determined by the mass relations [12,32]

$$\begin{aligned} \tan^2\theta_{^3P_1} &= \frac{4m_{K_{1A}}^2 - m_{a_1}^2 - 3m_{f_1(1420)}^2}{-4m_{K_{1A}}^2 + m_{a_1}^2 + 3m_{f_1(1285)}^2}, \\ \tan^2\theta_{^1P_1} &= \frac{4m_{K_{1B}}^2 - m_{b_1}^2 - 3m_{h_1(1380)}^2}{-4m_{K_{1B}}^2 + m_{b_1}^2 + 3m_{h_1(1170)}^2}, \end{aligned} \tag{3.17}$$

derived from the Gell-Mann-Okubo mass formula, where $m_{K_{1A,1B}}$ can be inferred from Eq. (3.2) with $\theta_{K_1} = 50.8°$. The signs of these angles can be determined from [12,32]

$$\begin{aligned} \tan\theta_{^3P_1} &= \frac{4m_{K_{1A}}^2 - m_{a_1}^2 - 3m_{f_1(1420)}^2}{2\sqrt{2}(m_{a_1}^2 - m_{K_{1A}}^2)}, \\ \tan\theta_{^1P_1} &= \frac{4m_{K_{1B}}^2 - m_{b_1}^2 - 3m_{h_1(1380)}^2}{2\sqrt{2}(m_{b_1}^2 - m_{K_{1B}}^2)}. \end{aligned} \tag{3.18}$$

Denoting the mass of the $\bar{s}s$ component as $m_{s\bar{s}}$, we have

$$m_{s\bar{s}}^2 = m_{f'}^2\sin^2\alpha + m_f^2\cos^2\alpha. \tag{3.19}$$

The obtained $m_{s\bar{s}}$ for various states are summarized in Table V.

TABLE IV. Branching fractions for the radiative decays $B \to K^*\gamma$, $K_1(1270)\gamma$, $K_1(1400)\gamma$, $K_2^*(1430)\gamma$ (in units of 10^{-5}) in the covariant light-front model and in other models. Experimental data are taken from Sec. I.

	$B^- \to K^{*-}\gamma$	$B^- \to K_1(1270)^-\gamma$	$B^- \to K_1(1400)^-\gamma$	$B^- \to K_2^*(1430)^-\gamma$
Experiment	4.21 ± 0.18	4.3 ± 1.2	<1.5	1.45 ± 0.43
This work	$4.28^{+2.78}_{-1.46}$	$5.12^{+1.72}_{-1.77}$ [a] $1.26^{+0.99}_{-0.38}$ [b]	$0.79^{+0.76}_{-0.25}$ [a] $4.50^{+1.53}_{-1.60}$ [b]	$2.94^{+3.18}_{-1.39}$
Lattice [35]	$2.99^{+2.97}_{-1.13}$ [c]			
Relativistic quark model [38]	8.2 ± 2.7 [d]	0.45 ± 0.15	0.78 ± 0.18	1.7 ± 0.6
Light front quark model [39]	$6.46^{+2.22}_{-1.15}$ [e]			
LCSR [40]	3.52 ± 1.41 [f]	0.71 ± 0.28 [f]	0.32 ± 0.14 [f]	1.76 ± 0.71 [f]
LCSR [22]	$3.22^{+2.38}_{-1.01}$ [g]	$6.6^{+3.7}_{-3.0}$ [h]	$0.65^{+1.28}_{-0.63}$ [h]	
AP [21]	6.8 ± 2.6			
BFS [15]	$7.4^{+0.8}_{-0.9}$ [i]			
BB [16]	$7.4^{+2.6}_{-2.4}$ [j]			
BJZ [41]	5.33 ± 1.47			
HQET [42]	9.99 ± 3.81 [d]	1.52 ± 0.56 [f]	0.74 ± 0.32 [f]	2.18 ± 1.02 [f]
SCET [43]	4.6 ± 1.4			
pQCD [44]	$3.58^{+1.84}_{-1.35}$			

[a]For the $K_1(1270)$–$K_1(1400)$ mixing angle $\theta_{K_1} = 50.8°$.
[b]For the $K_1(1270)$–$K_1(1400)$ mixing angle $\theta_{K_1} = -44.8°$.
[c]Use of $T_1(0) = 0.24^{+0.05}_{-0.03}$ [35] has been made.
[d]The original result is scaled up by a factor of $|a_7(K^*\gamma)/c_7^{\rm eff}|^2 = 1.78$.
[e]Use of $T_1(0) = 0.36$ [39] has been made.
[f]Use has been made of $\mathcal{B}(b \to s\gamma) = 3.52 \times 10^{-4}$ [7].
[g]Use of $T_1(0) = 0.25^{+0.03}_{-0.02}$ [22] has been made.
[h]For $\theta_{K_1} = 34 \pm 13°$ in our sign convention for $|K_1(1270)\rangle$ and $|K_{1B}\rangle$ states.
[i]The central value and errors are taken from the complete NLO result for the neutral mode.
[j]For $T_1(0) = 0.38$.

Defining $\langle 0|\bar{s}\gamma_\mu\gamma_5 s|s\bar{s}\rangle = m_{s\bar{s}} f^s \varepsilon_\mu$ and $\langle 0|\bar{s}\gamma_\mu\gamma_5 s|f\rangle = m_f f_f^s \varepsilon_\mu$, it follows from Eq. (3.15) that

$$m_{f'} f_{f'}^s = -m_{s\bar{s}} f^s \sin\alpha, \qquad m_f f_f^s = m_{s\bar{s}} f^s \cos\alpha. \quad (3.20)$$

From the values of α and $m_{s\bar{s}}$ shown in Table V and the decay constants of $f_1(^3P_1)$ and $f_8(^3P_1)$ determined to be -245 ± 13 MeV and -239 ± 13 MeV, respectively, in [45], we obtain $f^s(^3P_1) = f^s_{f(1420)} m_{f(1420)}/(-m_{s\bar{s}}\sin\alpha) = -230 \pm 9$ MeV,[5] which is the decay constant of the $^3P_1$ axial-vector meson with a pure $s\bar{s}$ quark content. Consequently, $\beta_{f_1,s\bar{s}}$ is determined and shown in Table I. For p-wave mesons, we take for simplicity $\beta_{f_1,s\bar{s}} = \beta_{h_1,s\bar{s}} = \beta_{f_2,s\bar{s}}$ [28]. Input parameters relevant to $B_s \to M\gamma$ decays are summarized in Table I.

Tensor form factors for $B_s \to V, A(^3P_1), A(^1P_1), T(^3P_2)$ transitions are shown in Table VI. As in the B decay case, except for the form factors Y_{B3} and $U_{2,3}$, the momentum dependence of the form factors T_i, $Y_{Ai,Bi}$, U_i are fitted to the 3 parameter form given in Eq. (3.10) with m_B replaced by m_{B_s}, while $Y_{B3}(q^2)$, $U_2'(q^2)$, and $U_3(q^2)$ are fitted to the form shown in Eq. (3.11) with m_B replaced by m_{B_s}, as well. Recall that U_2' is defined through Eq. (3.12). These form factors are plotted in Fig. 3. Comparing Tables II and VI, we notice that the values of form factors at $q^2 = 0$ are similar to the corresponding ones in B transitions. Therefore, flavor of the spectator quark does not seem to play a special role in these radiative B and B_s decays.

Form factors for $B_s \to f_1, h_1, f_2^{(\prime)}$ transitions with physical final states can be obtained from Table VI by including suitable Clebsch-Gordan coefficients. Specifically, form factors for various $B_s \to M$ transitions with $i = 1, 2, 3$ are given by

$$\begin{aligned} Y_{f_1(1420)i} &= -\sin\alpha_{^3P_1} \times Y_{Ai}, \\ Y_{f_1(1285)i} &= \cos\alpha_{^3P_1} \times Y_{Ai}, \\ Y_{h_1(1380)i} &= -\sin\alpha_{^1P_1} \times Y_{Bi}, \\ Y_{h_1(1170)i} &= \cos\alpha_{^1P_1} \times Y_{Bi}, \\ Y_{f_2'(1525)i} &= -\sin\alpha_{^3P_2} \times U_i, \\ Y_{f_2(1270)i} &= \cos\alpha_{^3P_2} \times U_i. \end{aligned} \quad (3.21)$$

TABLE V. Summary on mixing angles and $m_{s\bar{s}}$, obtained from Eqs. (3.17) and (3.19), for various isosinglet p-wave mesons [12,32].

$^{2s+1}l_J$	f'	f	$\alpha(°)$	$m_{s\bar{s}}$ (GeV)
$^1P_1$	$h_1(1380)$	$h_1(1170)$	54.7	1.32
$^3P_1$	$f_1(1420)$	$f_1(1285)$	94.9	1.43
$^3P_2$	$f_2'(1525)$	$f_2(1270)$	84.3	1.52

[5]Using $f^s(^3P_1) = f^s_{f(1285)} m_{f(1285)}/(m_{s\bar{s}}\cos\alpha)$, a similar central value is obtained, but the error is of order 100 MeV.

TABLE VI. Same as Table II except for the tensor form factors of $B_s \to \phi$, $f_1^{(\prime)}$, $h_1^{(\prime)}$, f_2 transitions. Note that Clebsch-Gordan coefficients are not included (see the text for more details).

F	$F(0)$	$F(q^2_{\rm max})$	a	b	F	$F(0)$	$F(q^2_{\rm max})$	a	b
T_1	0.27	0.72	1.99	1.58	Y_{A1}	0.36	1.07	1.70	0.89
T_2	0.27	0.91	1.17	0.18	Y_{A2}	0.36	0.58	0.67	−0.06
T_3	0.16	0.40	1.54	0.96	Y_{A3}	0.23	0.35	0.90	0.48
Y_{B1}	0.12	0.29	1.98	1.73	U_1	0.28	0.55	2.30	2.65
Y_{B_2}	0.12	0.28	1.17	0.37	U_2[a]	0.28	0.78	···	···
Y_{B3}[b]	−0.09	−0.24	2.23	0.01	U_2'[a]	0.29	0.45	2.10	2.75
					U_3[b]	−0.18	−0.55	2.74	0.07

[a]We use $U_2 \equiv U_1 + (q^2/m^2_{B_s})U_2'$ and fit for U_2' using Eq. (3.10).
[b]Y_{B3} and U_3 are fitted using Eq. (3.11).

Since only the $s\bar{s}$ components of these mesons can be transited from a B_s meson via a $\bar{b}\sigma_{\mu\nu}s$ density, the sizes of the corresponding form factors are reduced by the Clebsch-Gordan coefficients [see also Eq. (3.15)].

For the effective Wilson coefficient a_7, we shall use the QCDF ones as shown in Eqs. (2.8) and (2.9) with input parameters given in Appendix B.

Rates of radiative $B_s \to \phi\gamma$, $f_1(1420)\gamma$, $f_1(1285)\gamma$, $h_1(1380)\gamma$, $h_1(1170)\gamma$, $f_2'(1525)\gamma$, $f_2(1270)\gamma$ decays can be obtained in analog to the B meson case. Results obtained by using tensor form factors calculated in the covariant light-front model are shown in Table VII where comparison with results from other models [41,43,44] and data [11] is also made. We see that the calculated $B_s \to \phi\gamma$ rate is consistent with the data [11] and other models [41,43,44] within errors. Note that our $B_s \to \phi\gamma$ branching fraction is smaller than the $B \to K^*\gamma$ one. The branching fraction of $B_s \to \phi\gamma$ can be related to the $B \to K^*\gamma$ one via

$$\mathcal{B}(B_s \to \phi\gamma) = \left(\frac{m_B}{m_{B_s}}\right)^3 \left(\frac{m^2_{B_s} - m^2_\phi}{m^2_B - m^2_{K^*}}\right)^3 \frac{\tau(B_s)}{\tau(B)} \times \left|\frac{a_7^c(\phi\gamma)T_1^{B_s\phi}(0)}{a_7^c(K^*\gamma)T_1^{BK^*}(0)}\right|^2 \mathcal{B}(B \to K^*\gamma) \simeq 0.914 \left|\frac{T_1^{B_s\phi}(0)}{T_1^{BK^*}(0)}\right|^2 \mathcal{B}(B \to K^*\gamma). \quad (3.22)$$

It is clear that the reduction arises from the fact that $T_1(0)$

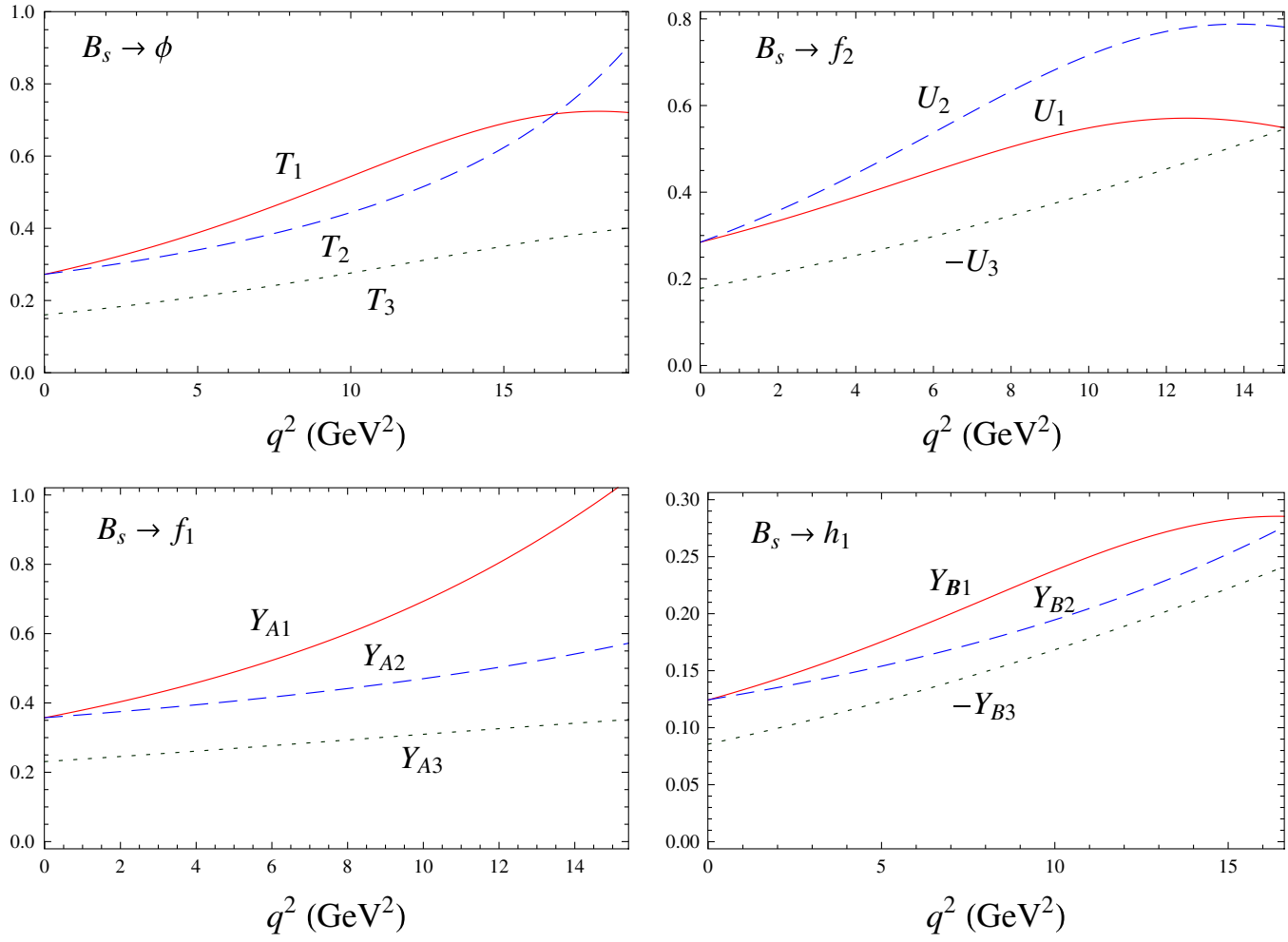

FIG. 3 (color online). Same as Fig. 2 except for $B_s \to M$ transitions.

TABLE VII. Branching fractions for the radiative decays $B_s \to \phi\gamma$, $f_1(1420)\gamma$, $f_1(1285)\gamma$, $h_1(1380)\gamma$, $h_1(1170)\gamma$, $f_2'(1525)\gamma$, $f_2(1270)\gamma$ (in units of 10^{-5}) in the covariant light-front model and other models. Experimental data are from [7,11].

	$B_s \to \phi\gamma$	$B_s \to f_1(1420)\gamma$	$B_s \to f_1(1285)\gamma$	$B_s \to h_1(1380)\gamma$
Experiment	$5.7^{+2.1}_{-1.8}$			
This work	$3.39^{+2.45}_{-1.22}$	$4.81^{+1.55}_{-1.17}$	$0.03^{+0.11}_{-0.01}$	$0.27^{+0.14}_{-0.15}$
BJZ [41]	3.94 ± 1.19			
SCET [43]	4.3 ± 1.4			
pQCD [44]	$3.58^{+1.46}_{-1.09}$	$6.19^{+3.06\,a}_{-2.52}$ $5.82^{+2.88\,b}_{-2.38}$	$0.01^{+0.01\,a}_{-0.01}$ $0.38^{+0.18\,b}_{-0.14}$	$4.44^{+2.09\,c}_{-1.66}$ $5.00^{+2.22\,d}_{-1.85}$
	$B_s \to h_1(1170)\gamma$	$B_s \to f_2'(1525)\gamma$	$B_s \to f_2(1270)\gamma$	
This work	$0.15^{+0.07}_{-0.08}$	$2.30^{+2.19}_{-0.99}$	$0.04^{+0.04}_{-0.02}$	
pQCD [44]	$0.79^{+0.36\,c}_{-0.28}$ $0.23^{+0.12\,d}_{-0.01}$			

[a]For the mixing angle $\theta_{^3P_1} = 38°$.
[b]For the mixing angle $\theta_{^3P_1} = 50°$.
[c]For the mixing angle $\theta_{^1P_1} = 10°$.
[d]For the mixing angle $\theta_{^1P_1} = 45°$.

for the $B_s \to \phi$ transition is smaller than that for the $B \to K^*$ one by 7% and the ratio of B_s and B lifetimes $\tau(B_s)/\tau(B) \simeq 0.87$ [12] leads to a further suppression.

Branching fractions for $B_s \to f_1(1420)\gamma$ and $f_2'(1525)\gamma$ are predicted to reach the level of 10^{-5}. It will be interesting to search for these modes in the near future. Comparing to other predictions, we note that most of our results on $B_s \to A\gamma$ decays agree with those in [44] except the one in $B_s \to h_1(1380)\gamma$ decay, where our result is about 1 order of magnitude smaller. Our predictions on $B_s \to f_1(1420)\gamma$, $f_1(1285)\gamma$, $h_1(1380)\gamma$, $h_1(1170)\gamma$, $f_2'(1525)\gamma$, $f_2(1270)\gamma$ rates can also be checked in future experiments.

IV. CONCLUSION

$B \to M$ and $B_s \to M$ tensor form factors are calculated in the covariant light-front quark model. All numerical results are analyzed using the CLF formulas in [17] with previously missing terms being included (see the second reference of [17]). Exclusive radiative B and B_s decays, $B \to K^*\gamma$, $K_1(1270)\gamma$, $K_1(1400)\gamma$, $K_2^*(1430)\gamma$ and $B_s \to f_1(1420)\gamma$, $f_1(1285)\gamma$, $h_1(1380)\gamma$, $h_1(1170)\gamma$, $f_2'(1525)\gamma$, $f_2(1270)\gamma$, are obtained using QCDF. Our main conclusions are as follows:

(1) The treatment on $m_{K_{1A}}$ and $m_{K_{1B}}$ is improved. In [17] these masses were determined with some approximations from the measured masses of $K_1(1270)$, $K_1(1400)$, $b_1(1232)$, and $h_1(1380)$ and no information of the mixing angle was used. In the present work, we use Eq. (3.2) to determine these masses. This procedure does not rely on any approximation.

(2) The treatment on the $K_{1A} - K_{1B}$ mixing angle θ_{K_1} is also improved. In [17], θ_{K_1} was taken to be ± 37 and ± 58 degrees from other analyses. These analyses were either based on the assumption of a vanishing decay constant of K_{1B} or relied on some other calculated results of $f_{K_{1A}}$. Since the formalism employed in this work is capable of providing information on $f_{K_{1A}}$ and $f_{K_{1B}}$, we can analyze the mixing angle consistently within the covariant light-front approach.

(3) $B \to V\gamma$ and $A\gamma$ decay rates are obtained using the QCDF approach with form factors calculated in this work. The predictions on $B \to A\gamma$ rates are more reliable than that in [17], where only a naïve estimation on the effective Wilson coefficients was used.

(4) The updated $B \to K_1(1270)\gamma$ rate is in agreement with the data, while the $B \to K_1(1400)\gamma$ rate is consistent with the experimental bound [8]. These decay rates are very sensitive to the $K_1(1270)$–$K_1(1400)$ mixing angle, and we found that $\theta_K = 50.8°$ is favored by the data.

(5) The predicted $B \to K^*\gamma$ and $K_2\gamma$ rates agree with data.

(6) The calculated $B_s \to \phi\gamma$ rate agree with experiment, though in the lower end of the data.

(7) In addition, we have studied all $B_s \to (A, T)\gamma$ decays with $b \to s$ transition. Branching fractions of $B_s \to f_1(1420)\gamma$ and $f_2'(1525)\gamma$ are predicted to reach the level of 10^{-5}. It will be interesting to search for these modes. Our predictions on $f_1(1285)\gamma$, $h_1(1380)\gamma$, $h_1(1170)\gamma$, $f_2(1270)\gamma$ decay rates can also be checked in future experiments.

ACKNOWLEDGMENTS

H. Y. C. wishes to thank the hospitality of the Physics Department, Brookhaven National Laboratory. This research was supported in part by the National Science Council of R.O.C. under Grants No. NSC97-2112-M-001-004-MY3 and No. NSC97-2112-M-033-002-MY3.

APPENDIX A: A BRIEF DERIVATION OF ANALYTICAL EXPRESSIONS OF TENSOR FORM FACTORS

In this appendix, we give a brief derivation that leads to the analytic formulas of tensor form factors given in [17]. We consider the transition amplitude given by the one-loop diagram as shown in Fig. 1. The incoming (outgoing) meson has the momentum $P'^{(\prime\prime)} = p_1'^{(\prime\prime)} + p_2$, where $p_1'^{(\prime\prime)}$ and p_2 are the momenta of the off-shell quark and antiquark, respectively, with masses $m_1'^{(\prime\prime)}$ and m_2. These momenta can be expressed in terms of the internal variables $(x_i, p'_\perp)$,

$$p'^{+}_{1,2} = x_{1,2}P'^{+}, \qquad p'_{1,2\perp} = x_{1,2}P'_\perp \pm p'_\perp, \tag{A1}$$

with $x_1 + x_2 = 1$. Note that we use $P' = (P'^{-}, P'^{+}, P'_\perp)$, where $P'^{\pm} = P'^{0} \pm P'^{3}$, so that $P'^2 = P'^{+}P'^{-} - P'^2_\perp$. In the covariant light-front approach, total four momentum is conserved at each vertex where quarks and antiquarks are off-shell. It is useful to define some internal quantities:

$$\begin{aligned} M_0'^2 &= (e_1' + e_2)^2 = \frac{p_\perp'^2 + m_1'^2}{x_1} + \frac{p_\perp'^2 + m_2^2}{x_2}, \\ \tilde{M}_0' &= \sqrt{M_0'^2 - (m_1' - m_2)^2}, \\ e_i^{(\prime)} &= \sqrt{m_i^{(\prime)2} + p_\perp'^2 + p_z'^2}, \\ p_z' &= \frac{x_2 M_0'}{2} - \frac{m_2^2 + p_\perp'^2}{2x_2 M_0'}. \end{aligned} \tag{A2}$$

Here, $M_0'^2$ can be interpreted as the kinetic invariant mass squared of the incoming $q\bar{q}$ system, and e_i the energy of the quark i.

We need Feynman rules for the meson-quark-antiquark vertices to calculate the amplitudes depicted in Fig. 1. The Feynman rules for vertices $(i\Gamma'_M)$ of ground-state s-wave mesons and low-lying p-wave mesons are summarized in Table VIII. Note that we use ^3A and ^1A to denote $^3P_1$ and $^1P_1$ states, respectively. It is known that the integration of the minus component of the internal momentum in Fig. 1 will force the antiquark to be on its mass shell [18]. The specific form of the (phenomenological) covariant vertex functions for on-shell quarks can be determined by comparing to the conventional vertex functions [19].

TABLE VIII. Feynman rules for the vertices $(i\Gamma'_M)$ of the incoming mesons-quark-antiquark, where p_1' and p_2 are the quark and antiquark momenta, respectively. Under the contour integrals to be discussed below, H'_M and W'_M are reduced to h'_M and w'_M, respectively, whose expressions are given by Eq. (A10). Note that for outgoing mesons, we shall use $i(\gamma_0\Gamma'^{\dagger}_M\gamma_0)$ for the corresponding vertices.

$M(^{2S+1}L_J)$	$i\Gamma'_M$
Pseudoscalar $(^1S_0)$	$H'_P\gamma_5$
Vector $(^3S_1)$	$iH'_V[\gamma_\mu - \frac{1}{W'_V}(p'_1 - p_2)_\mu]$
Axial $(^3P_1)$	$-iH'_{^3A}[\gamma_\mu + \frac{1^V}{W'_V}(p'_1 - p_2)_\mu]\gamma_5$
Axial $(^1P_1)$	$-iH'_{^1A}[\frac{1}{W'_A}(p'^{^3A}_1 - p_2)_\mu]\gamma_5$
Tensor $(^3P_2)$	$i\frac{1}{2}H'_T[\gamma_\mu - \frac{1}{W'_V}(p'_1 - p_2)_\mu](p'_1 - p_2)_\nu$

We first consider the tensor form factors for $B_q \to V$ transition. We have

$$\begin{aligned} \mathcal{B}_{\mu\nu}\varepsilon^{\prime\prime *\nu} &\equiv \langle V(P'', \varepsilon'')|\bar{s}\sigma_{\mu\lambda}q^\lambda(1+\gamma_5)b|\bar{B}_q(P')\rangle \\ &= -i^3\frac{N_c}{(2\pi)^4}\int d^4p_1'\frac{H'_P(iH''_V)}{N'_1N''_1N_2}S_{R\mu\nu}\varepsilon^{\prime\prime *\nu}, \end{aligned} \tag{A3}$$

where

$$\begin{aligned} S_{R\mu\nu} = \mathrm{Tr}\Big[&\Big(\gamma_\nu - \frac{1}{W''_V}(p''_1 - p_2)_\nu\Big)(\not{p}''_1 + m''_1)\sigma_{\mu\lambda} \\ &\times q^\lambda(1+\gamma_5)(\not{p}'_1 + m'_1)\gamma_5(-\not{p}_2 + m_2)\Big], \end{aligned} \tag{A4}$$

$N''_1 = p''^2_1 - m''^2_1 + i\epsilon$ and $N_2 = p_2^2 - m_2^2 + i\epsilon$. By using the identity $2\sigma_{\mu\lambda}\gamma_5 = i\epsilon_{\mu\lambda\rho\sigma}\sigma^{\rho\sigma}$, the above trace $S_{R\mu\nu}$ can be further decomposed into

$$S_{R\mu\nu} = q^\lambda S_{\nu\mu\lambda} + \frac{i}{2}q^\lambda\epsilon_{\mu\lambda\rho\sigma}S_\nu^{\rho\sigma}. \tag{A5}$$

It is straightforward to show that

$$\begin{aligned} S_{\nu\mu\lambda} = {}& 2\epsilon_{\mu\nu\alpha\lambda}[2(m'_1m_2 + m''_1m_2 - m'_1m''_1)p'^{\alpha}_1 + m'_1m''_1P^\alpha + (m'_1m''_1 - 2m'_1m_2)q^\alpha] - \frac{1}{W''_V}(4p'_{1\nu} - 3q_\nu - P_\nu) \\ &\times \epsilon_{\mu\lambda\alpha\beta}[(m'_1 + m''_1)p'^{\alpha}_1P^\beta + (m''_1 - m'_1 + 2m_2)p'^{\alpha}_1q^\beta + m'_1P^\alpha q^\beta] + \{2\epsilon_{\mu\nu\alpha\lambda}[2(p'_1\cdot p_2 - p''_1\cdot p_2 - p'_1\cdot p''_1)p'^{\alpha}_1 \\ &+ p'_1\cdot p''_1P^\alpha + (-2p'_1\cdot p_2 + p'_1\cdot p''_1)q^\alpha] + 2(g_{\lambda\nu}\epsilon_{\mu\alpha\beta\rho} - g_{\mu\nu}\epsilon_{\lambda\alpha\beta\rho})P^\alpha q^\beta p'^{\rho}_1 + 2\epsilon_{\lambda\mu\alpha\beta}(P^\alpha q^\beta p'_{1\nu} + p'^{\alpha}_1P^\beta q_\nu \\ &+ q^\alpha p'^{\beta}_1P_\nu) + 2\epsilon_{\mu\nu\alpha\beta}[p'_{1\lambda}P^\alpha q^\beta + q_\lambda P^\alpha p'^{\beta}_1 + (P+2q)_\lambda q^\alpha p'^{\beta}_1 + 2p'_{1\lambda}p'^{\alpha}_1(P+q)^\beta] \\ &- 2\epsilon_{\lambda\nu\alpha\beta}[p'_{1\mu}P^\alpha q^\beta + q_\mu P^\alpha p'^{\beta}_1 + (P+2q)_\mu q^\alpha p'^{\beta}_1 + 2p'_{1\mu}p'^{\alpha}_1(P+q)^\beta]\}. \end{aligned} \tag{A6}$$

Note that those terms in $\{\cdots\}$ are missed in the original version of [17]. To proceed, it is useful to use the following identities:

$$
\begin{aligned}
2p_1' \cdot p_2 &= M'^2 - p_1'^2 - p_2^2 = M'^2 - N_1' - N_2 - m_1'^2 - m_2^2, \\
2p_1'' \cdot p_2 &= M''^2 - p_1''^2 - p_2^2 = M''^2 - N_1'' - N_2 - m_1''^2 - m_2^2, \\
2p_1' \cdot p_1'' &= -q^2 + p_1'^2 - p_1''^2 = -q^2 + N_1' + N_1'' + m_1'^2 + m_1''^2.
\end{aligned} \tag{A7}
$$

As in [18,19], we shall work in the $q^+ = 0$ frame. For the integral in Eq. (A3), we perform the p_1^- integration [18], which picks up the residue at $p_2 = \hat{p}_2$ and leads to

$$
\begin{gathered}
N_1^{\prime(\prime\prime)} \to \hat{N}_1^{\prime(\prime\prime)} = x_1(M^{\prime(\prime\prime)2} - M_0^{\prime(\prime\prime)2}), \qquad H_M^{\prime(\prime\prime)} \to h_M^{\prime(\prime\prime)}, \qquad W_M'' \to w_M'', \\
\int \frac{d^4 p_1'}{N_1' N_1'' N_2} H_P' H_V'' S \to -i\pi \int \frac{dx_2 d^2 p_\perp'}{x_2 \hat{N}_1' \hat{N}_1''} h_P' h_V'' \hat{S},
\end{gathered} \tag{A8}
$$

where

$$
M_0''^2 = \frac{p_\perp''^2 + m_1''^2}{x_1} + \frac{p_\perp''^2 + m_2^2}{x_2}, \tag{A9}
$$

with $p_\perp'' = p_\perp' - x_2 q_\perp$. The explicit forms of h_M' and w_M' are given by [19]

$$
\begin{aligned}
h_P' &= h_V' = (M'^2 - M_0'^2)\sqrt{\frac{x_1 x_2}{N_c}} \frac{1}{\sqrt{2}\tilde{M}_0'} \varphi', \qquad h_{3A}' = (M'^2 - M_0'^2)\sqrt{\frac{x_1 x_2}{N_c}} \frac{1}{\sqrt{2}\tilde{M}_0'} \frac{\tilde{M}_0'^2}{2\sqrt{2}M_0'} \varphi_p', \\
h_{1A}' &= h_T' = (M^{2\prime} - M_0'^2)\sqrt{\frac{x_1 x_2}{N_c}} \frac{1}{\sqrt{2}\tilde{M}_0'} \varphi_p', \qquad w_V' = M_0' + m_1' + m_2, \qquad w_{3A}' = \frac{\tilde{M}_0'^2}{m_1' - m_2}, \qquad w_{1A}' = 2,
\end{aligned} \tag{A10}
$$

where φ' and φ_p' are the light-front momentum distribution amplitudes for s-wave and p-wave mesons, respectively. The Gaussian-type wave function is used [46]

$$
\varphi' = \varphi'(x_2, p_\perp') = 4\left(\frac{\pi}{\beta'^2}\right)^{3/4} \sqrt{\frac{dp_z'}{dx_2}} \exp\left(-\frac{p_z'^2 + p_\perp'^2}{2\beta'^2}\right), \qquad \varphi_p' = \varphi_p'(x_2, p_\perp') = \sqrt{\frac{2}{\beta'^2}} \varphi', \qquad \frac{dp_z'}{dx_2} = \frac{e_1' e_2}{x_1 x_2 M_0'}. \tag{A11}
$$

The parameter β' is expected to be of order $\Lambda_{\rm QCD}$.

In general, $\hat{p}_1'$ can be expressed in terms of three external vectors, P', q, and $\tilde{\omega}$ [$\tilde{\omega}$ being a lightlike vector with the expression $\tilde{\omega}^\mu = (\tilde{\omega}^-, \tilde{\omega}^+, \tilde{\omega}_\perp) = (2, 0, 0_\perp)$]. In practice, for $\hat{p}_1'$ under integration we use the following rules [18]:

$$
\begin{aligned}
\hat{p}_{1\mu}' &\doteq P_\mu A_1^{(1)} + q_\mu A_2^{(1)}, \qquad \hat{p}_{1\mu}' \hat{p}_{1\nu}' \doteq g_{\mu\nu} A_1^{(2)} + P_\mu P_\nu A_2^{(2)} + (P_\mu q_\nu + q_\mu P_\nu) A_3^{(2)} + q_\mu q_\nu A_4^{(2)}, \\
\hat{p}_{1\mu}' \hat{p}_{1\nu}' \hat{p}_{1\alpha}' &\doteq (g_{\mu\nu} P_\alpha + g_{\mu\alpha} P_\nu + g_{\nu\alpha} P_\mu) A_1^{(3)} + (g_{\mu\nu} q_\alpha + g_{\mu\alpha} q_\nu + g_{\nu\alpha} q_\mu) A_2^{(3)} + P_\mu P_\nu P_\alpha A_3^{(3)} \\
&\quad + (P_\mu P_\nu q_\alpha + P_\mu q_\nu P_\alpha + q_\mu P_\nu P_\alpha) A_4^{(3)} + (q_\mu q_\nu P_\alpha + q_\mu P_\nu q_\alpha + P_\mu q_\nu q_\alpha) A_5^{(3)} + q_\mu q_\nu q_\alpha A_6^{(3)}, \\
\hat{N}_2 &\doteq Z_2, \qquad \hat{p}_{1\mu}' \hat{N}_2 \doteq q_\mu \left[A_2^{(1)} Z_2 + \frac{P \cdot q}{q^2} A_1^{(2)} \right],
\end{aligned} \tag{A12}
$$

where the symbol $\doteq$ reminds us that the above equations are true only after integration. In the above equation, $A_j^{(i)}$ and Z_2 are functions of $x_{1,2}$, $p_\perp'^2$, $p_\perp' \cdot q_\perp$, and q^2, and their explicit expressions are given by [18]

$$
\begin{aligned}
A_1^{(1)} &= \frac{x_1}{2}, \qquad A_2^{(1)} = A_1^{(1)} - \frac{p_\perp' \cdot q_\perp}{q^2}, \qquad A_1^{(2)} = -p_\perp'^2 - \frac{(p_\perp' \cdot q_\perp)^2}{q^2}, \qquad A_2^{(2)} = (A_1^{(1)})^2, \\
A_3^{(2)} &= A_1^{(1)} A_2^{(1)}, \qquad A_4^{(2)} = (A_2^{(1)})^2 - \frac{1}{q^2} A_1^{(2)}, \qquad A_1^{(3)} = A_1^{(1)} A_1^{(2)}, \qquad A_2^{(3)} = A_2^{(1)} A_1^{(2)},
\end{aligned} \tag{A13}
$$

$$A_3^{(3)} = A_1^{(1)}A_2^{(2)}, \qquad A_4^{(3)} = A_2^{(1)}A_2^{(2)},$$
$$A_5^{(3)} = A_1^{(1)}A_4^{(2)}, \qquad A_6^{(3)} = A_2^{(1)}A_4^{(2)} - \frac{2}{q^2}A_2^{(1)}A_1^{(2)},$$
$$Z_2 = \hat{N}_1' + m_1'^2 - m_2^2 + (1-2x)M'^2 + (q^2 + q\cdot P)\frac{p_\perp' q_\perp}{q^2}. \tag{A14}$$

The calculation for $B_q \to A_{^3P_1,{}^1P_1}$ transition form factors can be done in a similar manner. In analogue to Eq. (A3), we have

$$\mathcal{B}^{^3P_1}_{\mu\nu}\varepsilon^{\prime\prime *\nu} = -i^3\frac{N_c}{(2\pi)^4}\int d^4p_1' \frac{H_P'(-iH_{3A}'')}{N_1'N_1''N_2} S^{3A}_{R\mu\nu}\varepsilon^{\prime\prime *\nu},$$
$$\mathcal{B}^{^1P_1}_{\mu\nu}\varepsilon^{\prime\prime *\nu} = -i^3\frac{N_c}{(2\pi)^4}\int d^4p_1' \frac{H_P'(-iH_{1A}'')}{N_1'N_1''N_2} S^{1A}_{R\mu\nu}\varepsilon^{\prime\prime *\nu}, \tag{A15}$$

where

$$S^{^3A}_{R\mu\nu} = \mathrm{Tr}\Big[\Big(\gamma_\nu - \frac{1}{W_{^3A}''}(p_1''-p_2)_\nu\Big)\gamma_5(\not{p}_1'' + m_1'') \times \sigma_{\mu\lambda}q^\lambda(1+\gamma_5)(\not{p}_1' + m_1')\gamma_5(-\not{p}_2 + m_2)\Big],$$
$$S^{^1A}_{R\mu\nu} = \mathrm{Tr}\Big[\Big(-\frac{1}{W_{^1A}''}(p_1''-p_2)_\nu\Big)\gamma_5(\not{p}_1'' + m_1'') \times \sigma_{\mu\lambda}q^\lambda(1+\gamma_5)(\not{p}_1' + m_1')\gamma_5(-\not{p}_2 + m_2)\Big]. \tag{A16}$$

It can be easily shown that $S^{^3A,{}^1A}_{R\mu\nu} = -S_{R\mu\nu}$ with m_1'' and W_V'' replaced by $-m_1''$ and $W''_{^3A,{}^1A}$, respectively, while only the $1/W''_{^1A}$ term is kept for the $S^{^1A}_R$ case. Consequently, we have, for $i = 1, 2, 3$,

$$Y_{Ai,Bi}(q^2) = T_i(q^2) \quad \text{with} \quad (m_1'' \to -m_1'', h_V'' \to h''_{^3A,{}^1A}, w_V'' \to w''_{^3A,{}^1A}), \tag{A17}$$

where only the $1/W''$ terms in Y_{Bi} form factors are kept. It should be cautious that the replacement of $m_1'' \to -m_1''$ should not be applied to m_1'' in w'' and h''.

Finally, we turn to the $B_q \to T$ transition given by

$$\mathcal{B}^T_{\mu\nu\lambda}\varepsilon^{\prime\prime *\nu\lambda} \equiv \langle T(P'',\varepsilon'')|\bar{s}\sigma_{\mu\nu}(1+\gamma_5)q^\nu b|\bar{B}_q(P')\rangle = -i^3\frac{N_c}{(2\pi)^4}\int d^4p_1' \frac{H_P'(-iH_T'')}{N_1'N_1''N_2} S^{PT}_{\mu\nu\lambda}\varepsilon^{\prime\prime *\nu\lambda}, \tag{A18}$$

where

$$S^T_{R\mu\nu\lambda}\varepsilon^{\prime\prime *\nu\lambda}(p'') \equiv S_{R\mu\nu}\frac{(p_2 - p_1'')_\lambda}{2}\varepsilon^{\prime\prime *\nu\lambda}(p'') = S_{R\mu\nu}(q - p_1')_\lambda\varepsilon^{\prime\prime *\nu\lambda}(p''). \tag{A19}$$

The contribution from the $S_{\mu\nu}q_\lambda$ part is trivial, since q_λ can be taken out from the integration, which is already done in the $B_q \to V$ case. Contributions from the $\hat{S}_{R\mu\nu}\hat{p}'_{1\lambda}$ part can be worked out by using Eq. (A12).

The final results of these calculations, i.e. tensor form factors for $B_q \to M$ transitions, are given in [17] and recollected in Sec. II.

APPENDIX B: INPUT PARAMETERS FOR DECAY AMPLITUDES IN THE QCDF APPROACH

Input parameters of the radiative B decay amplitudes are collected in Table IX. Values of form factors are calculated in this work. Other hadronic parameters are from [12,22,41,45]. Note that the signs of $f_M^\perp$ for $M = {}^1P_1$ states are flipped to match our sign convention. For Gegenbauer moments of physical mesons, we use

TABLE IX. Input parameters. The values of the scale dependent quantities $f^\perp(\mu_h)$ and $a^\perp_{0,1,2}(\mu_h)$ are given for $\mu_h = 1$ GeV.

Light mesons				
M	$f_M^\perp$ (MeV)	$a_0^\perp$	$a_1^\perp$	$a_2^\perp$
K^* [41]	185 ± 10	1	0.04 ± 0.03	0.15 ± 0.15
ϕ [41]	186 ± 9	1	0	0.2 ± 0.2
K_{1A} [22]	250 ± 13	$0.26^{+0.03}_{-0.22}$	-1.08 ± 0.48	0.02 ± 0.20
K_{1B} [22]	-190 ± 10	1	$0.30^{+0.00}_{-0.31}$	-0.02 ± 0.22
$f_1^{^3P_1}$ [45]	245 ± 13	0	-1.06 ± 0.36	0
$f_8^{^3P_1}$ [45]	239 ± 13	0	-1.11 ± 0.31	0
$h_1^{^1P_1}$ [45]	-180 ± 12	1	0	0.18 ± 0.22
$h_8^{^1P_1}$ [45]	-190 ± 10	1	0	0.14 ± 0.22

B mesons [12]				
B	m_B (GeV)	τ_B (ps)	f_B (MeV)	λ_B (MeV)
B_u	5.279	1.638	200 ± 15	350 ± 100
B_s	5.366	1.472	230 ± 15	350 ± 100

Form factors $F^{B\to M}(0)$ (this work)			
$T_1^{B\to K^*}(0)$	$Y_{A1}^{B\to K_{1A}}(0)$	$Y_{B1}^{B\to K_{1B}}(0)$	$U_1^{B\to K_2}(0)$
0.29 ± 0.03	0.36 ± 0.02	0.13 ± 0.01	0.28 ± 0.03
$T_1^{B_s\to\phi}(0)$	$Y_{A1}^{B_s\to f_{^3P_1}^s}(0)$	$Y_{B1}^{B_s\to h_{^1P_1}^s}(0)$	$U_1^{B\to f_{^3P_2}^s}(0)$
0.27 ± 0.03	0.36 ± 0.02	0.12 ± 0.01	0.28 ± 0.03

Quark masses [12]	
$m_b(m_b)$/GeV	m_c/m_b
$4.20^{+0.17}_{-0.07}$	0.31

CKM matrix elements [27]	
$\lvert V_{cb}\rvert$	$\lvert V_{cs}\rvert$
$0.04117^{+0.00038}_{-0.00117}$	$0.97349^{+0.00018}_{-0.00017}$

$$a_i^{\perp,K_1(1270)} = \frac{f_{K_{1A}}^\perp}{f_{K_1(1270)}^\perp} a_i^{\perp,K_{1A}} \sin\theta_K + \frac{f_{K_{1B}}^\perp}{f_{K_1(1270)}^\perp} a_i^{\perp,K_{1A}} \cos\theta_K, \quad a_i^{\perp,K_1(1400)} = \frac{f_{K_{1A}}^\perp}{f_{K_1(1400)}^\perp} a_i^{\perp,K_{1A}} \cos\theta_K - \frac{f_{K_{1B}}^\perp}{f_{K_1(1400)}^\perp} a_i^{\perp,K_{1A}} \sin\theta_K,$$
$$a_i^{\perp,f^s} = \frac{f_{f_1}^\perp}{f_f^\perp} a_i^{\perp,f_1} \frac{\cos\theta}{\sqrt{3}} - 2\frac{f_8^\perp}{f_f^\perp} a_i^{\perp,f_8} \frac{\sin\theta}{\sqrt{6}}, \quad a_i^{\perp,f'^s} = -\frac{f_1'^\perp}{f_{f'}^\perp} a_i^{\perp,f_1'} \frac{\sin\theta}{\sqrt{3}} - 2\frac{f_8'^\perp}{f_{f'}^\perp} a_i^{\perp,f_2'} \frac{\cos\theta}{\sqrt{6}}, \tag{B1}$$

with

$$f_{K_1(1270)}^\perp = f_{K_{1A}}^\perp \sin\theta_K + f_{K_{1B}}^\perp \cos\theta_K, \quad f_{K_1(1400)}^\perp = f_{K_{1A}}^\perp \cos\theta_K - f_{K_{1B}^\perp}^\perp \sin\theta_K,$$
$$f_{f^s}^\perp = f_{f_1}^\perp \frac{\cos\theta}{\sqrt{3}} - 2f_{f_8}^\perp \frac{\sin\theta}{\sqrt{6}}, \quad f_{f'^s}^\perp = -f_{f_1'}^\perp \frac{\sin\theta}{\sqrt{3}} - 2f_{f_8'}^\perp \frac{\cos\theta}{\sqrt{6}}, \tag{B2}$$

where $\theta = \alpha - 54.7°$ and f, f' are the states specified in Table V. The scale μ for a_7^c is varied from $m_b/2$ to $2m_b$.

[1] T. Aaltonen *et al.* (CDF Collaboration), Phys. Rev. Lett. **100**, 161802 (2008).
[2] V. M. Abazov *et al.* (D0 Collaboration), Phys. Rev. Lett. **101**, 241801 (2008).
[3] R. Ammar *et al.* (CLEO Collaboration), Phys. Rev. Lett. **71**, 674 (1993).
[4] T. E. Coan *et al.* (CLEO Collaboration), Phys. Rev. Lett. **84**, 5283 (2000).
[5] B. Aubert *et al.* (*BABAR* Collaboration), Phys. Rev. Lett. **103**, 211802 (2009).
[6] M. Nakao *et al.* (Belle Collaboration), Phys. Rev. D **69**, 112001 (2004).
[7] E. Barberio *et al.* (Heavy Flavor Averaging Group Collaboration), arXiv:0808.1297 and online update, [http://www.slac.stanford.edu/xorg/hfag/].
[8] H. Yang *et al.* (Belle Collaboration), Phys. Rev. Lett. **94**, 111802 (2005).
[9] S. Nishida *et al.* (Belle Collaboration), Phys. Rev. Lett. **89**, 231801 (2002).
[10] B. Aubert *et al.* (*BABAR* Collaboration), Phys. Rev. D **70**, 091105 (2004).
[11] J. Wicht *et al.* (Belle Collaboration), Phys. Rev. Lett. **100**, 121801 (2008).
[12] C. Amsler *et al.* (Particle Data Group), Phys. Lett. B **667**, 1 (2008).
[13] P. Ball and V. M. Braun, Phys. Rev. D **58**, 094016 (1998).
[14] M. Beneke, G. Buchalla, M. Neubert, and C. T. Sachrajda, Phys. Rev. Lett. **83**, 1914 (1999); Nucl. Phys. **B591**, 313 (2000).
[15] M. Beneke, T. Feldmann, and D. Seidel, Eur. Phys. J. C **41**, 173 (2005); Nucl. Phys. **B612**, 25 (2001).
[16] S. W. Bosch and G. Buchalla, Nucl. Phys. **B621**, 459 (2002); S. W. Bosch, arXiv:hep-ph/0208203; S. W. Bosch and G. Buchalla, in *Proceedings of the Second Workshop on the CKM Uniatrity Triangle*, edited by P. Ball *et al.* (Durham, United Kingdom, 2003).
[17] H. Y. Cheng and C. K. Chua, Phys. Rev. D **69**, 094007 (2004); **81**, 059901(E) (2010).
[18] W. Jaus, Phys. Rev. D **60**, 054026 (1999).
[19] H. Y. Cheng, C. K. Chua, and C. W. Hwang, Phys. Rev. D **69**, 074025 (2004).
[20] C. W. Hwang and Z. T. Wei, J. Phys. G **34**, 687 (2007); C. W. Hwang, Eur. Phys. J. C **62**, 499 (2009); Y. L. Shen and Y. M. Wang, Phys. Rev. D **78**, 074012 (2008); W. Wang, Y. L. Shen, and C. D. Lu, Eur. Phys. J. C **51**, 841 (2007); Phys. Rev. D **79**, 054012 (2009).
[21] A. Ali and A. Ya. Parkhomenko, Eur. Phys. J. C **23**, 89 (2002).
[22] H. Hatanaka and K. C. Yang, Phys. Rev. D **77**, 094023 (2008); **78**, 059902(E) (2008).
[23] W. Jaus, Phys. Rev. D **44**, 2851 (1991); **53**, 1349 (1996); **54**, 5904(E) (1996).
[24] W. Jaus, Phys. Rev. D **67**, 094010 (2003).
[25] C. W. Hwang, Eur. Phys. J. C **23**, 585 (2002).
[26] H. Y. Cheng, C. Y. Cheung, and C. W. Hwang, Phys. Rev. D **55**, 1559 (1997).
[27] J. Charles *et al.* (CKMfitter Group), Eur. Phys. J. C **41**, 1 (2005) and the online update, [http://ckmfitter.in2p3.fr/].
[28] D. Scora and N. Isgur, Phys. Rev. D **52**, 2783 (1995); N. Isgur, D. Scora, B. Grinstein, and M. B. Wise, Phys. Rev. D **39**, 799 (1989).
[29] M. Suzuki, Phys. Rev. D **47**, 1252 (1993).
[30] L. Burakovsky and T. Goldman, Phys. Rev. D **56**, R1368 (1997).
[31] H. Y. Cheng, Phys. Rev. D **67**, 094007 (2003).
[32] H. Y. Cheng and K. C. Yang, Phys. Rev. D **76**, 114020 (2007); **78**, 094001 (2008).
[33] R. H. Li, C. D. Lu, and W. Wang, Phys. Rev. D **79**, 034014 (2009).
[34] K. C. Yang, Phys. Rev. D **78**, 034018 (2008).
[35] D. Becirevic, V. Lubicz, and F. Mescia, Nucl. Phys. **B769**, 31 (2007).
[36] R. H. Li, C. D. Lu, and W. Wang, Phys. Rev. D **79**, 034014 (2009).
[37] J. P. Lee, Phys. Rev. D **74**, 074001 (2006).
[38] D. Ebert, R. N. Faustov, V. O. Galkin, and H. Toki, Phys. Rev. D **64**, 054001 (2001).
[39] C. Q. Geng, C. W. Hwang, C. C. Lih, and W. M. Zhang, Phys. Rev. D **64**, 114024 (2001).
[40] A. S. Safir, Eur. Phys. J. C **15**, 1 (2001).

[41] P. Ball, G. W. Jones, and R. Zwicky, Phys. Rev. D **75**, 054004 (2007).
[42] S. Veseli and M. G. Olsson, Phys. Lett. B **367**, 309 (1996).
[43] A. Ali, B. D. Pecjak, and C. Greub, Eur. Phys. J. C **55**, 577 (2008).
[44] W. Wang, R. H. Li, and C. D. Lu, arXiv:0711.0432.
[45] K. C. Yang, Nucl. Phys. **B776**, 187 (2007).
[46] P. L. Chung, F. Coester, and W. N. Polyzou, Phys. Lett. B **205**, 545 (1988).